NAVAL POSTGRADUATE SCHOOL
Monterey, California

THESIS

DEVELOPMENT OF TELEMETRY FOR
THE AGILITY FLIGHT TEST OF
A RADIO CONTROLLED FIGHTER MODEL

by

Michael James Gallagher

March 1992

Thesis Advisor: Richard Howard

Approved for public release; distribution is unlimited.

Unclassified

Security Classification of this page

REPORT DOCUMENTATION PAGE

1a Report Security Classification: Unclassified	1b Restrictive Markings
2a Security Classification Authority	3 Distribution Availability of Report: Approved for public release; distribution is unlimited.
2b Declassification/Downgrading Schedule	
4 Performing Organization Report Number(s)	5 Monitoring Organization Report Number(s)
6a Name of Performing Organization: Naval Postgraduate School; 6b Office Symbol (*If Applicable*): AA	7a Name of Monitoring Organization: Naval Postgraduate School
6c Address (*city, state, and ZIP code*): Monterey, CA 93943-5000	7b Address (*city, state, and ZIP code*): Monterey, CA 93943-5000
8a Name of Funding/Sponsoring Organization; 8b Office Symbol (*If Applicable*)	9 Procurement Instrument Identification Number
8c Address (*city, state, and ZIP code*)	10 Source of Funding Numbers: Program Element Number; Project No; Task No; Work Unit Accession No

11 Title (*Include Security Classification*) DEVELOPMENT OF TELEMETRY FOR THE AGILITY FLIGHT TEST OF A RADIO CONTROLLED FIGHTER MODEL

12 Personal Author(s) Gallagher, Michael James

13a Type of Report	13b Time Covered	14 Date of Report (*year, month,day*)	15 Page Count
Master's Thesis	From To	March 1992	90

16 Supplementary Notation The views expressed in this thesis are those of the author and do not reflect the official policy or position of the Department of Defense or the U.S. Government.

17 Cosati Codes			18 Subject Terms (*continue on reverse if necessary and identify by block number*)
Field	Group	Subgroup	UAV, RPV, Telemetry, Supermaneuverability, Agility, Radio Control, High Angle of Attack.

19 Abstract (*continue on reverse if necessary and identify by block number*)

Advanced design tools, control devices, and supermaneuverability concepts provide innovative solutions to traditional aircraft design trade-offs. Emerging technologies enable improved agility throughout the performance envelope. Unmanned Air Vehicles provide an excellent platform for dynamic measurements and agility research. A 1/8-scaled F-16A ducted-fan radio-controlled aircraft was instrumented with a telemetry system to acquire angle of attack, sideslip angle, control surface deflection, throttle position, and airspeed data. A portable ground station was built to record and visually present real-time telemetry data. Flight tests will be conducted to acquire baseline high angle-of-attack performance measurements, and follow-on research will evaluate agility improvements with varied control configurations.

20 Distribution/Availability of Abstract	21 Abstract Security Classification
X unclassified/unlimited ___ same as report ___ DTIC users	Unclassified

Approved for public release; distribution is unlimited.

Development of Telemetry for the Agility Flight Test of a Radio Controlled Fighter Model

by

Michael James Gallagher
Lieutenant Commander, United States Navy
B.S., Oregon State University, 1978

Submitted in partial fulfillment of the requirements
for the degree of

MASTER OF SCIENCE IN AERONAUTICAL ENGINEERING

from the

NAVAL POSTGRADUATE SCHOOL

MARCH 1992

ABSTRACT

Advanced design tools, control devices, and supermaneuverability concepts provide innovative solutions to traditional aircraft design trade-offs. Emerging technologies enable improved agility throughout the performance envelope. Unmanned Air Vehicles provide an excellent platform for dynamic measurements and agility research. A 1/8-scaled F-16A ducted-fan radio-controlled aircraft was instrumented with a telemetry system to acquire angle of attack, sideslip angle, control surface deflection, throttle position, and airspeed data. A portable ground station was built to record and visually present real-time telemetry data. Flight tests will be conducted to acquire baseline high angle-of-attack performance measurements, and follow-on research will evaluate agility improvements with varied control configurations.

TABLE OF CONTENTS

LIST OF FIGURES

ACKNOWLEDGMENTS

On a thesis project of this scope it is necessary, but also rewarding, to seek the expertise and guidance of other professionals. I was extremely fortunate to find such professional assistance from a variety of fields. LCDR Chris Cleaver turned his F-16 thesis project over to me with excellent ideas and recommendations. Don Harvey contributed his years of metal craftsmanship to the design and construction of the alpha-beta "mousetrap." Don Meeks and Dave Eichstedt contributed a number of excellent recommendations on the restructuring of the F-16 model and the ground station. Mike Callaway provided his valuable, hands-on experience with flying ducted-fan models, answered numerous telephone questions about engine performance and fuel consumption, and waited patiently for flight tests to begin. Jack King kept the low-speed wind tunnel available for repeated airspeed calibration tests and was the source of countless electronic components for breadboard mock-ups of the telemetry system.

A special thanks is given to Tom Christian, electronics technician extraordinaire from the Mechanical Engineering Department. Tom was my only source of electronic "know-how," and despite an overwhelming workload he always found time to teach, guide, and enlighten. Without his personal interest and off-duty contributions, the airspeed and telemetry electronic designs would never have reached their final stages.

Finally, I owe a debt of gratitude to my thesis advisor, Professor Rick Howard, for his enthusiastic support and patient encouragement. When I strayed, he guided me to the right path; when I despaired, he was the source of hope; when I failed, he opened a new door to success.

I. INTRODUCTION

In a visual air-to-air engagement which commences from a position of mutual advantage, aircraft maneuverability is a key factor in the engagement outcome. Fighter aircraft design has evolved to provide speed and maneuverability improvements, but structural limitations and stability/control degradations have classically been obstacles to improvements in high angle-of-attack performance. These obstacles have necessitated the use of artificial angle-of-attack limiters in some aircraft which constrain the flight envelope and preclude loss of stability or control. Tactical emphasis has been placed on stand-off capabilities; tactical philosophy has maintained that "speed is life."

Frequently, however, an engagement will progress to close-in, aggressive maneuvering which can rapidly bring both aircraft into the low-speed, high angle-of-attack (high-α) flight regime. The necessity for aircraft to maneuver effectively in this regime has resulted in increased emphasis on high maneuverability and controllability, including the ability to perform rapid, transient maneuvers at high angles of attack with brief excursions into post-stall conditions. [Ref. 1:p. 279] Several emerging technologies, such as vectored thrust, digital flight controls, computational aerodynamics, vortex control, composite structures, and high thrust/weight engines have recently made it possible to explore the high-α flight regime. These technologies provide the opportunity to expand flight envelopes and employ new operational tactics to achieve dominant advantages in close-in-combat flight scenarios.

Recent studies which have investigated the potentials of these emerging technologies make frequent reference to aircraft "agility." Pilots consider an agile

aircraft as one which is able to "outpoint" an opponent, maintain prolonged high turn rates without sacrificing energy, and accelerate quickly out of a slow engagement with impunity or to regain maneuvering airspeed. [Ref. 2:p. 37] In his article on the subject, Dorn points out that this relatively new performance term has not been rigorously defined, but warrants both a clear scientific definition and detailed follow-on comparisons as aircraft designs are modified to implement advanced technology. While "agility" has variously been used with references to more conventional concepts as controllability, maneuverability, pointing ability, acceleration, dynamics, flying qualities, and performance, Dorn recommends that it be quantified as changes-in-state-per-unit-time. [Ref. 3:p. 2] Figure 1 illustrates the increased agility requirements of modern air combat vehicles.

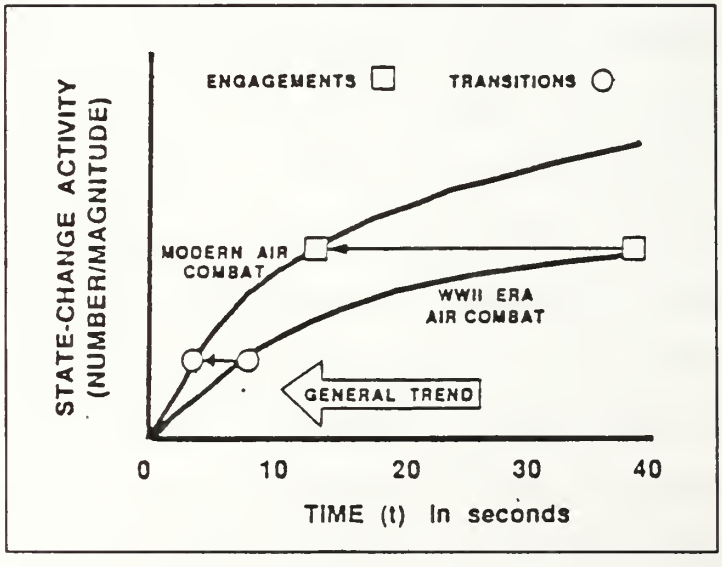

Figure 1: Trends in Fighter Combat [Ref. 3:p. 2]

Essentially, Dorn suggests that the complex realities of modern air warfare -- detection, visual or radar acquisition, maneuvering, weapons employment, etc.– call for a new scientifically based philosophy (a new scientific method) to realize potential advantages. While conventional performance parameters use similar time scales -- velocity, turn rate, roll rate, alpha dot, Ps vs. airspeed, etc. -- agility metrics could be defined and applied to multiple parameter changes-in-state with a variety of time scales. Two possible examples with different time scales are (1) loaded rolls and (2) spatial-state-change vs. energy-state-change. Loaded rolls at present are habitually avoided by pilots because rolling about the longitudinal axis at high angles-of-attack generates large sideslip excursions due to kinematic coupling, leading to high speed or high 'g' departure. This restriction in controllability requires unloading, rolling, then reloading the aircraft in series. Technology advances may be applied to increase an aircraft's ability to perform loaded rolls in a parallel maneuver (simultaneous state changes about different axes), providing a clear advantage to close-in-combat maneuvering and rolling pull-outs from bomb runs (Figure 2).

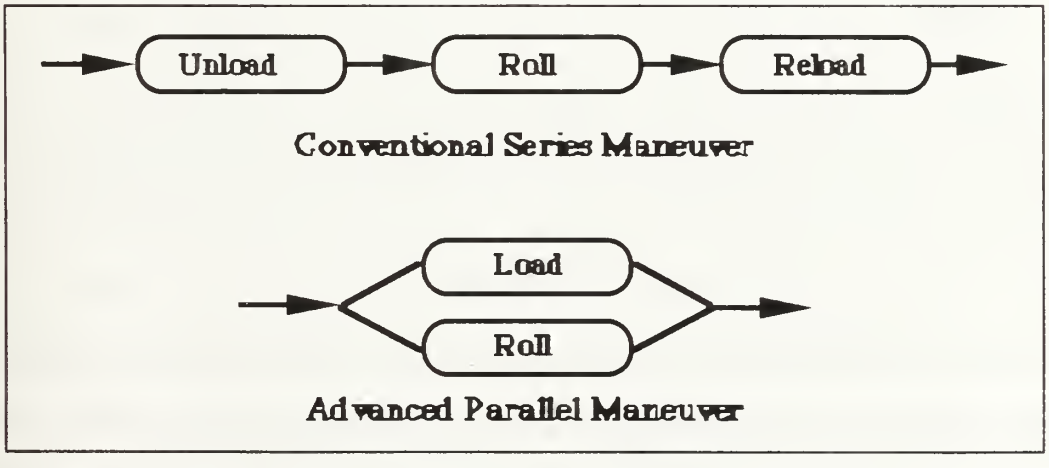

Figure 2: Loaded Rolls

In the case of spatial-state-change vs. energy-state-change, if a pilot could (a) point his nose to 70° AOA, shoot his opponent, unload, and reattain his initial speed in several seconds (Figure 3A), or (b) decelerate, load and bring his velocity vector to bear on the opponent, then unload and re-accelerate in several seconds (Figure 3B), a clear tactical advantage would be achieved, particularly in multiple aircraft engagements [Ref. 3:pp. 4,5].

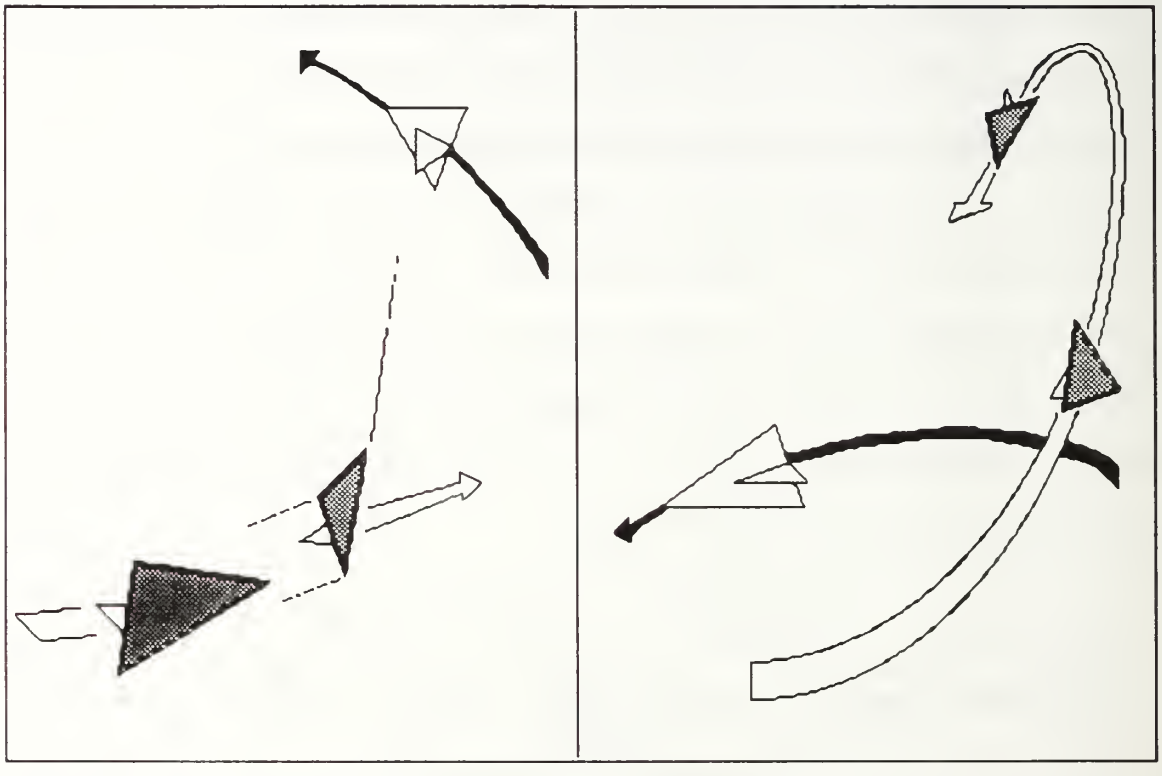

Figure 3A: Pointing Maneuver

Figure 3B: Positioning Maneuver

[Ref. 5:p. 13]

A rigorous methodology in the analysis of aircraft agility would also provide aircraft designers clearer guidelines and fresh perspectives to resolve largely contradictory design requirements. A persistent fighter design dilemma has

included the contradictory requirements of supersonic intercept, superiority against a larger number of maneuvering offensive targets with short-range weapons, and low take-off and landing speeds for either short field or carrier operations [Ref. 4:p. 1]. The designer was required to compromise relatively efficient supersonic configurations to comply with low-speed, high-α stability-and-control requirements [Ref. 5:p.3]. Analysis of agility based upon state-change-per-time provides the opportunity to factor in to design those characteristics which either (a) improve agility by decreasing the time to change a single aircraft state, or (b) increase the number of states that can be changed (possibly simultaneously) within a given period of time [Ref. 3:p. 4].

Three avenues of research have demonstrated promise in improving agility characteristics: Digital Fly-By-Wire Control, Delta Wing/Coupled Canard Designs, and Supermaneuverability Concepts.

A. DIGITAL FLY-BY-WIRE CONTROL

This technology has become state of the art. It allows multiple control surfaces to be simultaneously displaced in order to achieve and maintain a commanded flight condition compared to traditional mechanical systems which link control surface deflection to control stick displacement. This equates to an increase in the number of state variables available in an agility metric. Additionally, digital fly-by-wire program parameters may be modified to target specific mission-oriented flight modes. [Ref. 4:pp. 561,562] A revolutionary advantage that digital fly-by-wire provides is the capability to provide basic stability to an inherently unstable, and therefore highly maneuverable, design. The F-16 is a standard example of an aircraft design that employs this technology; the forward-swept-wing X-29A research aircraft is an extreme example. [Ref. 6:p. 2]

B. DELTA WING/CLOSE-COUPLED CANARD DESIGN

The advent of digital control systems and computational aerodynamics has revived interest in the delta wing. Computational aerodynamic modelling has enabled refinements to be made in wing planform, profile, twist distribution, and leading edge suction. The result has been a delta wing which maintains its classically good supersonic performance without sacrificing cruise or subsonic performance. When integrated with a close-coupled canard, optimized lift to drag is possible throughout the flight envelope and a method is provided for gust alleviation. [Ref. 4:pp. 562-563] The low wing loading of delta wings improves agility by reducing the time scale to perform changes-in-state; a delta-canard configuration improves agility by increasing the number of state variables available in an agility metric. Four current designs that employ delta-wing/close-coupled canards are the European Fighter Aircraft (EFA), France's Rafale, the Israeli Lavi, and Sweden's JAS-39 Gripen. All of these designs are strikingly similar. Low wing loading also complements supermaneuverability technologies. The X-31 research aircraft being jointly developed by the United States and West Germany combines digital control, a delta wing, a forward canard, and thrust vectoring into a futuristic agile fighter design [Ref. 7:pp. 58-60].

C. SUPERMANEUVERABILITY CONCEPTS

"Supermaneuverability" is a term applied to several concepts which allow controlled tactical maneuvers beyond maximum lift angles-of-attack or which influence the ability of an aircraft to yaw and pitch independent of the flight path vector. In the 30-50 degree angle-of-attack regime, the modern slender forebody fighter may experience unpredictable yawing moments due to the formation of

asymmetric vortices on the forebody. Conventional control surfaces, which are blanked by the stalled wing wake, may have insufficient control power to overcome these moments. The forebody, however, remains in undisturbed flow and the moment arm from the forebody to the cg is equal to or greater than the moment arm from the vertical tails (Figure 4). [Ref.1:p.280] The NASA High-Alpha Technology Program (HATP) has been investigating the nature of steady and unsteady separated flows, particularly vortex flows, using wind tunnel experiments, computational aerodynamics, piloted simulation, and flight tests with the modified F/A-18 High-Alpha Research Vehicle (HARV) [Ref. 5:p. 5].

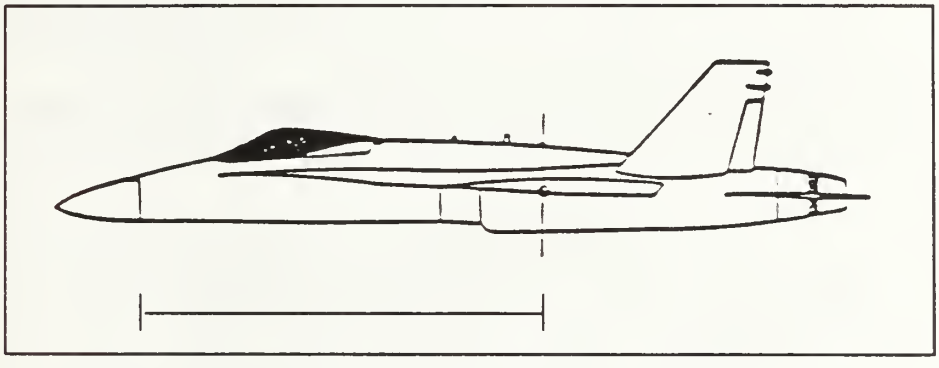

Figure 4: Fighter Forebody Moment Arm [Ref. 1:p. 286]

As the nature of separated vortex flows is better understood, methods may be applied to effectively manipulate or create such flows for enhanced control at high-α. Two schemes which have been researched are the use of variable forebody strakes (Figures 5A and 5B) and a number of forebody jet blowing techniques (Figure 6).

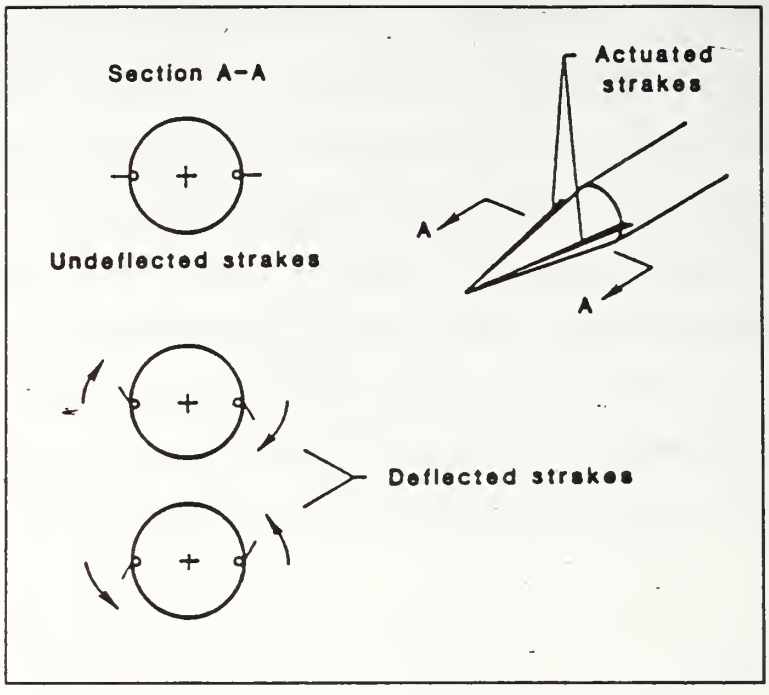

Figure 5A: Forebody Non-Conformal Strakes [Ref. 1:p. 286]

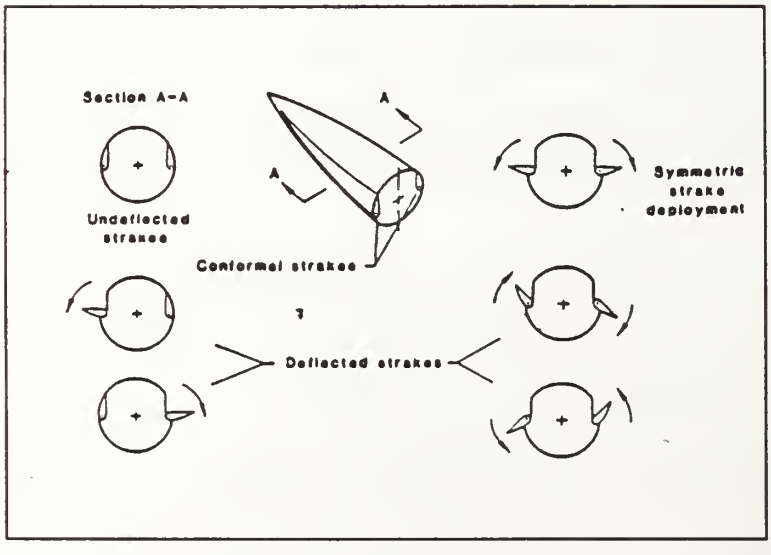

Figure 5B: Forebody Conformal Strakes [Ref. 1:p. 286]

Reznick and Flores have found good quantitative and qualitative agreement between Navier-Stokes solutions, wind-tunnel pressure-distribution data, and water-tunnel dye-flow visualization tests on a wing-strake-fuselage configuration similar to the F-16A [Ref. 8:p. 294]. Murri and Rao have shown that actuated forebody strakes on a generic fighter model provided significant yaw control capability over a wide range of sideslips and at angles of attack up to about 70° [Ref. 1:p. 285]. Tavella, Schiff, and Cummings have demonstrated through Navier-Stokes solutions with an F/A-18 fuselage forebody that asymmetrical blowing from slots can produce corresponding yawing moments five times higher than would be obtained from lateral blowing jets without generating a large net rolling moment [Ref. 9:p. 6].

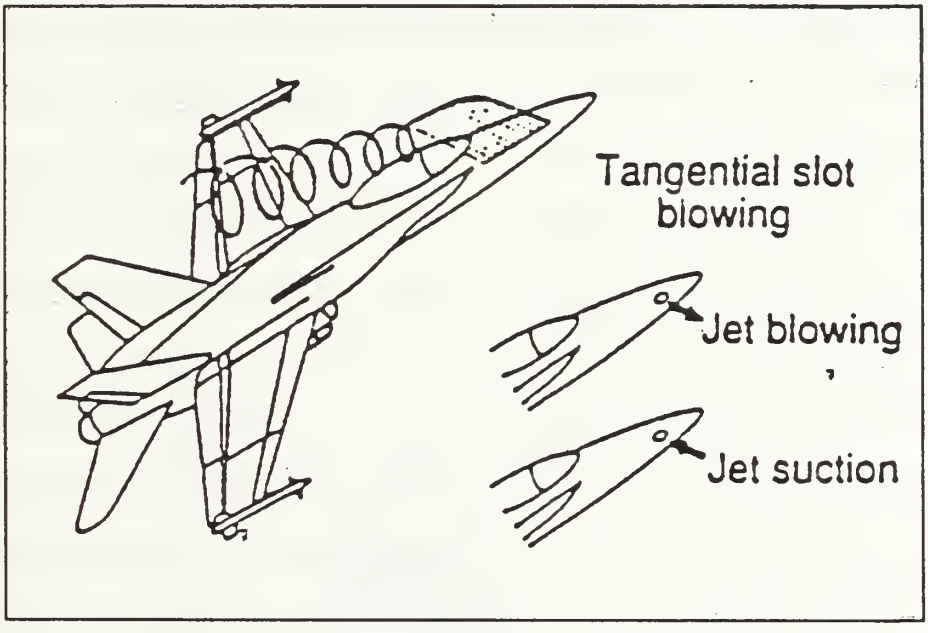

Figure 6: Forebody Jet Blowing Techniques [Ref. 5:p. 17]

The most suitable solution to post-stall maneuvering is vectored engine thrust. Beyond 50 degrees, the thrust vector becomes the dominant factor in maintaining controlled flight. [Ref. 4:p. 564] Vectored thrust technology could be integrated with digital control and would complement vortex control methods. The HARV is being modified to incorporate a simple multi-axis thrust-vectoring system (Figure 7); the same type of system is being used in the X-31 Program. [Ref. 5:p. 5] Perhaps the most ambitious thrust vectoring research is being conducted by McDonnell Douglas and the Air Force on a highly modified F-15B aircraft. Designated the S/MTD (Short Takeoff and Land/Maneuvering Technology Demonstrator), the aircraft features an integrated digital fly-by-wire/propulsion control system with a two-dimensional thrust reversing nozzle. Although current tests have focused primarily on short-field takeoff and landing performance, the flight test sequence is to include flight envelope expansion into the slow-speed, high-α regime and in-flight thrust reversal. [Ref. 10:pp. 73-76]

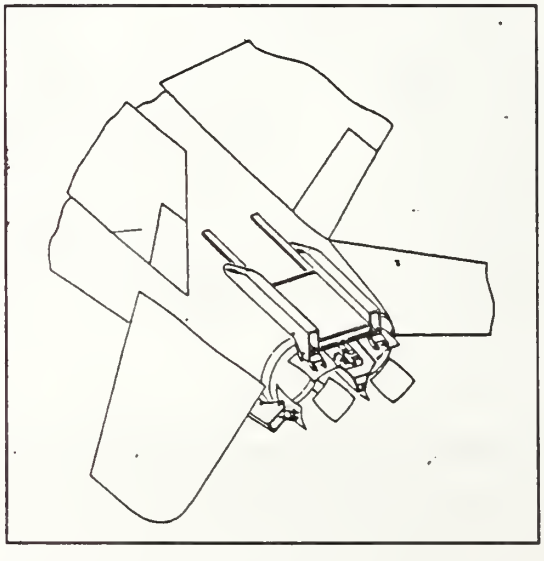

Figure 7: HARV/X-31 Thrust Vectoring Vanes [Ref. 5:p. 15]

D. USE OF RPVS IN AGILITY RESEARCH

An avenue of research into agility comparisons which has not been widely used is through construction and modification of unmanned air vehicles (UAVs) or remotely piloted vehicles (RPVs). Use of RPVs in research has not been fully explored, but it provides a viable and low-cost alternative to evaluate emerging technologies that is somewhere between ground-based wind tunnel and computational testing, simulation, and full-scale flight test. Several RPV research programs have provided excellent results, the most notable being the Highly Maneuverable Aircraft Technology (HiMAT) Program undertaken jointly by Rockwell Corporation and NASA [Ref. 11]. In Israel twelve prototype RPV designs have undergone wind tunnel tests and an RPV with two-dimensional thrust vectoring nozzles capable of ±20° pitch and ±35° yaw has been successfully test flown. The results have proven the practicality of the technology and its potential in larger manned aircraft. [Ref. 12:p. 21]

The Naval Postgraduate School's Department of Aeronautics and Astronautics is developing an Unmanned Air Vehicle Flight Research program with an established goal to achieve dynamic flight measurements and agility comparisons in the high-α flight regime using various models and configurations. A 1/7-scale F/A-18 dual ducted-fan model is currently being constructed and instrumented. A 1/8-scale ducted-fan, radio-controlled F-16A model has been constructed and successfully test flown. Instrumentation of this second model with a telemetry system for agility flight test is the topic of this thesis research.

II. SCOPE

A. UAV FLIGHT RESEARCH OBJECTIVES

The UAV flight research program in development at the Naval Postgraduate School has a broad scope, but several fundamental objectives:

- Applied aerodynamic engineering
- Applied design and configuration comparison
- Flight test support for both future UAV and future aircraft systems
- An avenue to perform comparative research which complements wind-tunnel and analytical computer-aided research

Areas of research which may be explored within the UAV program include:

- Fundamental Aerodynamics
- Stability and Control
- Propulsion
- Avionics
- Sensor Technology

Four fixed-wing UAV projects are currently in development or undergoing flight test:

- A 1/2-scale Pioneer is in flight test to determine baseline performance characteristics and low-speed handling qualities prior to modification,
- A 1/2-scale technology demonstrator, the Archytas TDF (Tilting Ducted Fan) has been constructed for research into vertical take-off and transition to horizontal flight studies,

- A commercially available 1/7-scale model of the F/A-18 is in construction for high-α and propulsion research, and
- A commercially available 1/8-scale model of the F-16A aircraft has been constructed for high-α research and instrumentation development.

The scaling effects of the commercially available models preclude exact similarity transformations of research results to their full-scale equivalents. These limitations include aeroelastic, dynamic, and kinematic similarities and Reynolds number matching. This does not, however, detract from the potential value of intended research; measurements resulting from configuration modifications may be compared to baseline measurements for each aircraft to determine agility improvements.

B. REQUIREMENTS FOR A TELEMETRY SYSTEM

It has been determined that a fundamental requirement for the future and potential of the UAV program is the development of a compact, light-weight, reliable, and flexible telemetry system. In all of the UAV projects, space limitations are a primary concern. Engines, unobstructed intake and exhaust ducts, fuel cells, retractable landing gear, servos, and radio control equipment consume the majority of available space, leaving little room for telemetry or other systems associated with future modifications. Weight restrictions are imposed by limited available thrust and center-of-gravity (cg) limitations. Flexibility is required so that a generic telemetry system may be used in each of the research platforms without major alterations to platform or system. A sturdy and reliable telemetry package is required to prevent possible signal interference, but also to withstand high frequency vibrations from engine operation and potentially heavy shocks from hard landings.

It has been found from experimental flight tests conducted to date on the Pioneer model that onboard data recording methods are inadequate. Engine vibration loads, particularly at high engine RPMs, have had a severe detrimental effect on the quality of recorded data. Attempts to isolate the recorder and damp the engine-induced structural vibrations have had limited success; however, data quality has remained unsatisfactory. [Ref. 13] A reliable telemetry system has been determined to be the simplest and most effective solution to these problems.

C. FINDING A SUITABLE TELEMETRY DESIGN

Investigation into the procurement of available telemetry systems from a variety of different sources has not been fruitful. Telemetry systems for small, light-weight scale models are not prevalent, and each system investigated has either exceeded in complexity the requirements of the UAV program, been too bulky to meet the limited space requirements, been too heavy for use in the various test models, and/or generally been too expensive in light of the relatively simple telemetry package needed.

The most promising solution to development of a simple telemetry system was judged to be the modification of commercially available radio-control (R/C) devices which are used by amateur model flyers. These devices are normally used to transmit command signals from a hand-held ground control unit to a receiver/servo system onboard the flying models. With appropriate modification, these same devices can be used to transmit airborne information from the aircraft back to a ground receiving station.

A seven-channel telemetry system suitable for use in the UAV program was developed from this context. The airborne portion of the system was installed in the F-16A model with appropriate instrumentation to detect angle of attack (alpha),

sideslip angle (beta), flight control deflections (stabilator, aileron, rudder), throttle position, and airspeed. A ground-based station was constructed to include a receiver and decoder, analog meters for direct visual feedback of each of the seven channels, and a data recorder. The ground station panel will be video recorded with appropriate verbal commentary during flight testing to describe flight sequence and maneuvers. The data recorder will be used to record transmitted data for subsequent digitization and computer-aided analysis.

The scope of the study was to provide "proof of concept" for the telemetry system as installed in the standard configuration F-16A model. Follow on flight tests will obtain agility comparisons of dynamic pitch rates and high-α yaw controllability. Further research with the F-16A model will include a complete baseline performance validation with the standard configuration, followed by agility studies with various configuration changes such as modified wing designs, canards, nose strakes, and possibly jet-blowing techniques.

III. TELEMETRY DEVELOPMENT

A. AIRBORNE TELEMETRY SYSTEM

The airborne telemetry system evolved from a number of electronic breadboard mock-ups and eventually emerged as a combination of commercially-available components and prototype components. The conceptual design of the system, however, remained essentially the same during the development process. Figure 8 shows the four fundamental components of the system: (1) low-torque potentiometers used to measure alpha, beta, control surface deflections, and throttle position (airspeed measurement required a special circuit, to be addressed later); (2) trimming potentiometers (TPot) to balance and calibrate inputs to the encoder; (3) a commercially-available encoder which converted potentiometer input voltages to a pulse-width-modulated (PWM) signal; and (4) a commercially-available transmitter to broadcast the PWM signal to the ground station.

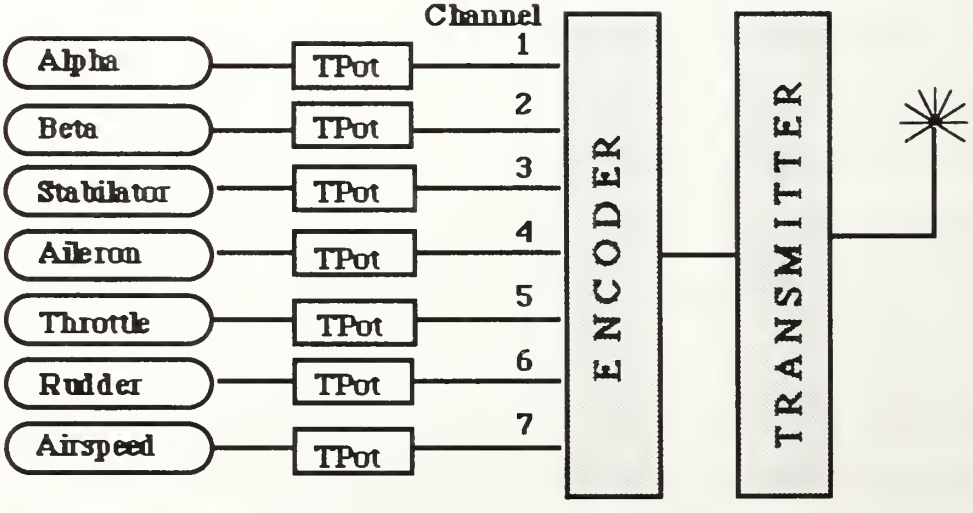

Figure 8: Airborne Telemetry Schematic

1. Encoder

At the heart of the airborne telemetry system was a programmable seven-channel encoding circuit obtained from a commercial source (model name Silver Seven). This encoder featured an IC multiplexer (NE 5044) which allowed from three to seven parallel inputs to be converted to generate a precise pulse-width-modulated signal. A dual linear ramp technique was used which provided excellent linearity, minimal crosstalk between channels, and low temperature drift. The IC multiplexer functioned as a strobed voltage follower which sampled each channel sequentially and transferred the input voltage to the output. Only one of the input channel voltages was actively sampled at a given time, and, when inactive, that input appearred as an open circuit. When active, each sample appearred as a high impedance input (>1MΩ), which eliminated input loading. Channel 4, 5, 6, or 7 inputs could be grounded to select the desired number of output pulses. For example, by grounding the channel 4 input, the chip could be used as a three-channel encoder; similarly, channels could be added on as required. The F-16A application made use of all seven channels.

Modulated output from the IC multiplexer was in the form of a seven-pulse code embedded within a 1.5 ms frame-width signal. As voltage inputs varied, their respective pulse-widths either elongated or contracted within this frame. The frame-width was variable (1.5 ± 0.5 ms); however, the factory-set width of 1.5 ms was found to be adequate.

The encoder featured an onboard 5-volt regulated source to drive external loads. During initial telemetry design no attempt was made to use this feature; attempts instead were made to use the flight control servo actuator output voltages as direct inputs to the encoder. Several adverse side-effects were noted

from these attempts: (1) feedback from the encoder to the control servos was occasionally experienced, making in-flight control of the aircraft susceptible to telemetry interference; (2) a buffering circuit was required for each control surface input to shield servos from this feedback; (3) the centering or reference voltage from each of the control servos was dissimilar, which would have necessitated precise calibration of each of the inputs; and (4) the servo output voltages were too low and of insufficient range to provide the level of accuracy desired in measuring control surface deflections. Thus, attempts to use servo output voltages were eventually abandoned because they required excessive electronic modification and components for input amplification, and because a potential existed for loss of inflight control of the model due to telemetry interference.

The subsequent design which utilized the encoder's reference supply voltage was considerably more efficient and less complex. With this design all potentiometers were supplied from the same 5-volt referenced source. As a result the circuitry and power supply required for inflight radio control of the aircraft were electrically isolated from the circuitry and power supply of the telemetry system.

The encoder, along with transmitter and airspeed electronics, was powered by a 9.6 VDC, 1200 mAh NiCad battery which was secured inside the aircraft's strakes adjacent to the cg.

2. Measurement of Alpha and Beta Deflections

Aircraft angle of attack (alpha) and sideslip angle (beta) were measured by alpha and beta vanes fabricated from brass rod and shim stock. Two alpha vanes protruded from the fuselage immediately forward of the strakes, one on either side

of the fuselage, so that at least one vane would remain in undisturbed flow during large yaw excursions. A single beta vane protruded from the fuselage underbelly 7-1/4" forward of the intake duct. Both vane sets were mechanically linked to 20kΩ low-torque (≤0.015 oz.-in.) potentiometers (Figure 9).

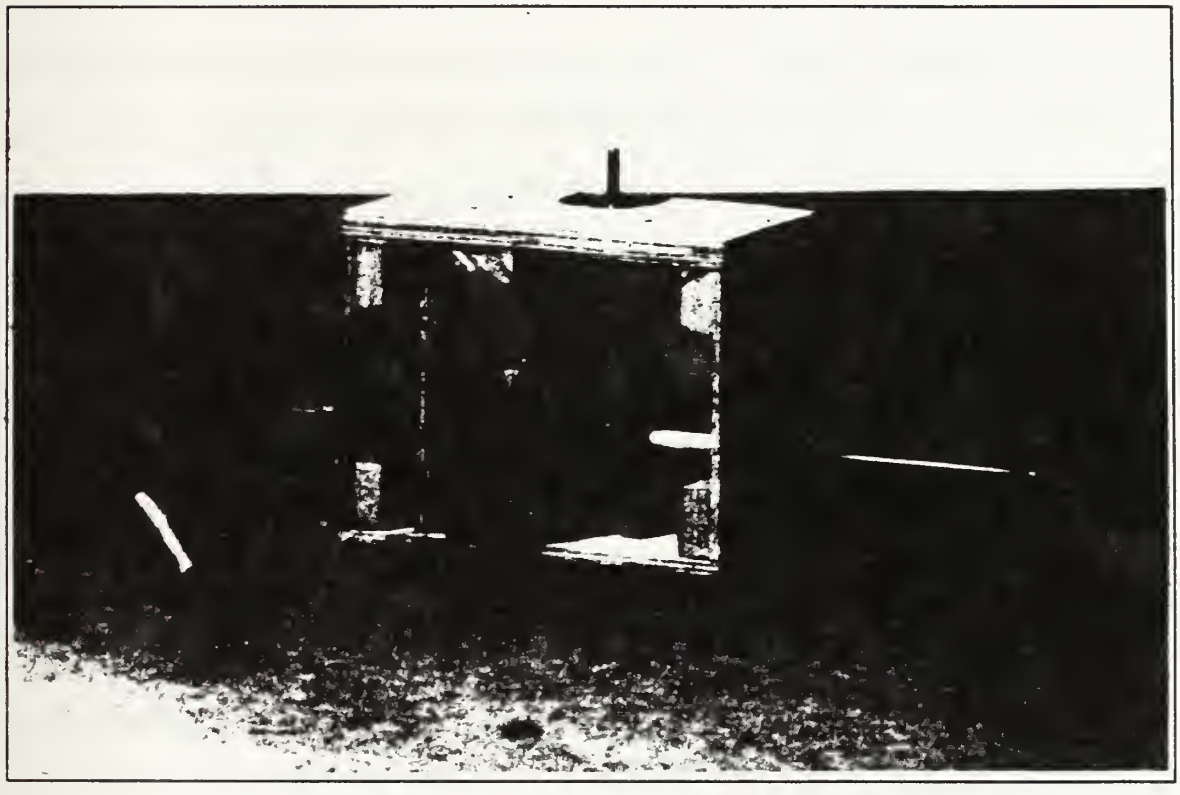

Figure 9: Alpha-Beta Framework (Inverted)

The alpha vane design featured a light-weight 1/4" aluminum rod which extended through the fuselage laterally and was mounted on ball bearings to a plywood veneer frame. The brass vanes attached to the aluminum rod on each side with set screws. Within the veneer frame a 1.3:1 plastic gear and pinion set transferred vane rotation to potentiometer displacement (Figure 10). This enabled 360 degrees of potentiometer displacement for 270 degrees of vane rotation,

increasing the sensitivity of measurement. The alpha potentiometer was inserted into the frame to mate the potentiometer pinion and vane gear. This arrangement was held in place by a spring and set screw to allow for fine adjustment and to prevent binding or backlash of the gears. The result was a sturdy, virtually frictionless device.

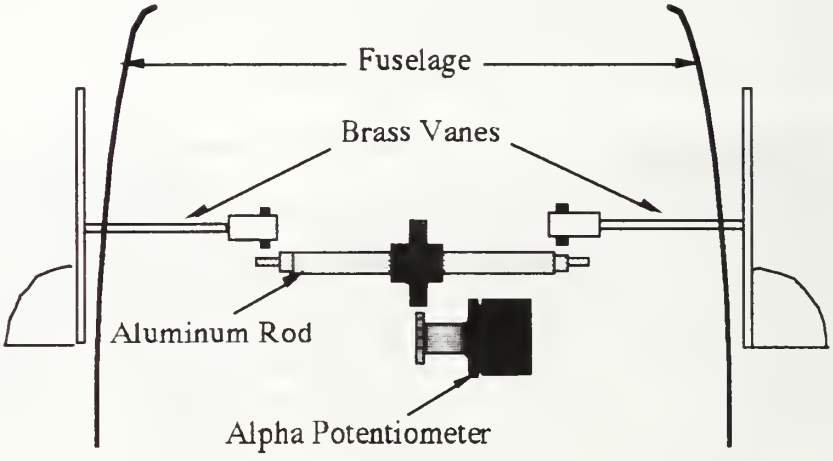

Figure 10: Alpha Measurement Device

The beta potentiometer was attached to the bottom of the alpha-beta framework, with its shaft protruding directly through the fuselage underbelly, and its vane attached directly with set screws.

Alpha and beta potentiometer wiper output voltages were routed to encoder channels 1 and 2, respectively, via 20kΩ trimming potentiometers. The trimming potentiometers allowed centerpoint voltages and ranges to be calibrated after the encoder was assembled.

3. Measurement of Control Surface Deflections and Throttle Position

Control surface deflections and throttle position were measured with potentiometers installed in the airframe at appropriate locations. Stabilator and starboard aileron 5kΩ potentiometers were mechanically linked to internal hardware which deflected those control surfaces. Space limitations required that rudder and throttle 10kΩ potentiometers be attached to their respective servos vice to the actual deflection hardware. This did not present a problem, however, because servo/control linkages were found to be free of play and potentiometers sufficiently sensitive that no measurable hysteresis was noted during calibration.

Stabilator, aileron, throttle position, and rudder potentiometer wiper output voltages were routed to encoder channels 3, 4, 5, and 6, respectively, via 10kΩ trimming potentiometers. Again, the trimming potentiometers allowed centerpoint voltages and ranges to be calibrated after the encoder was assembled.

4. Airspeed Measurement

Airspeed measurements were obtained from a square-tipped 1-3/4 inch diameter propeller which was boom-mounted on the top of the vertical fin. This high-speed sensor was obtained as a single component from a commercially-available remote-control airspeed system. The propeller was the only component of the system suitable for application to the project's airspeed indicator requirement, and featured a Cadmium-Sulfide (CdS) photo sensor facing the rear of the propeller (Figure 11). The indicator was rated for operation from 19 to 184 mph, which corresponded well with project requirements for an airspeed range from 30 mph at stall to approximately 130 mph at maximum level flight speed.

It was necessary to develop an electronic circuit capable of converting propeller RPM to an output voltage similar to the potentiometer output voltages (0--5 VDC). Four frequency-to-voltage breadboard designs were constructed and wind-tunnel tested before a suitable circuit was found. All designs were based upon use of a commercially-available frequency-to-voltage conversion chip (LM2917).

Figure 11: Airspeed Sensor

The principal difficulty with the initial designs was that the photosensor on the propeller provided a highly non-sinusoidal spiked signal as it was blocked during propeller blade passage. The tachometer circuit required a near-sinusoidal input signal. It was therefore necessary to modify the sensor signal through a high-

gain amplifier and use the resulting differentiated output as the input signal to the amplifier portion of the LM2917.

The amplified signal from the LM2917 was then fed to an RC combination charge pump (Figure 12: R1 and C1). The charge pump established a charging current proportional to the amplified input frequency which was then discharged from its capacitor (C1) through the resistor (R1) to obtain a pulse-modulated voltage at the input of the buffer amplifier section of the circuit.

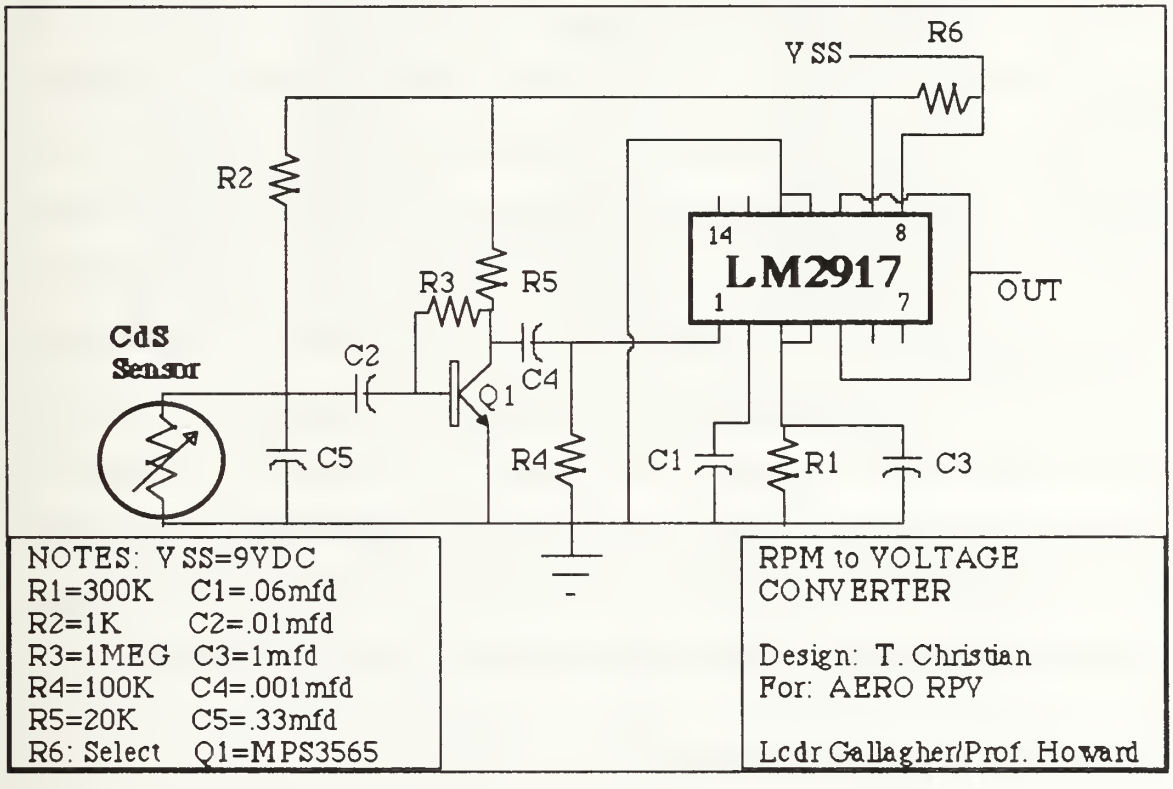

Figure 12: Airspeed Circuit Diagram

Capacitor C3 then integrated the pulses to provide a DC voltage level proportional to the input frequency. An RC combination of 300kΩ and 0.06μf was used to

obtain a full-scale frequency of 300 Hz (equivalent to approximately 135 mph) and full-scale output voltage of approximately 4.75 VDC.

5. Transmitter

The transmitter was obtained commercially as an assembled and tuned RF component of the Silver Seven package. Output from the encoder was input to the transmitter without modification. The transmitter frequency was 27.195 MHz, which was approved by the FCC for model aircraft application under the new 1991 FCC frequency regulations.

6. Airborne Telemetry Package

Trimming potentiometers, airspeed electronics, and Silver Seven encoder and transmitter were all mounted on a removable 24-contact circuitboard. This modularity allowed the circuitboard to be easily removed and installed as required in any of the research aircraft. A compact 26-pin connector provided input/output between the potentiometers and airspeed sensor installed in the F-16 model and the telemetry circuit. A 15-pin connector was included to provide access to encoder input voltages and the encoder output signal for bench-test calibration or calibration with the ground station. Two miniature toggle switches were installed in the F-16 to provide power to the encoder/airspeed circuits and the transmitter. The completely assembled airborne telemetry package weighed 0.52 lbs (8.3 oz.).

B. GROUND-BASED TELEMETRY SYSTEM

The ground-based portion of the telemetry system (Figure 13) was in principle the inverse of the airborne system. A Silver Seven receiver captured the airborne PWM signal for parallel decoding to analog meters and recorder. Several significant differences, however, existed between the airborne and ground-based electronics: (1) the Silver Seven receiver actually included an IC demodulator

(NE 5045) similar--but not identical--to the encoder's IC multiplexer (NE 5044); and (2) the output from the IC demodulator was not an analog signal. These differences presented a significant obstacle to successfully decoding transmitted data.

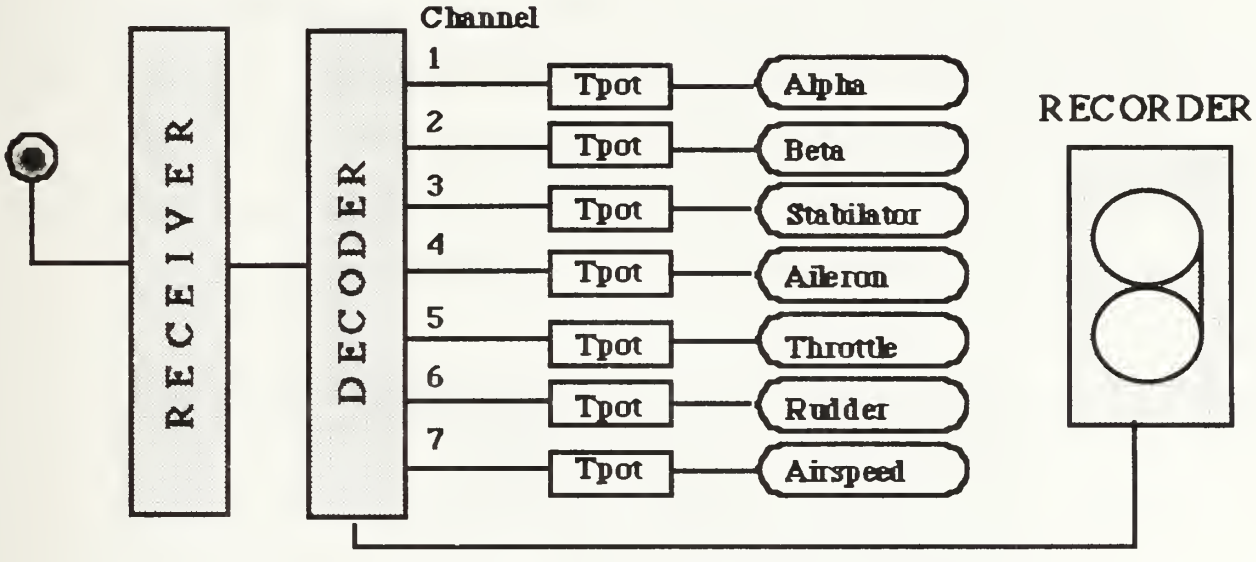

Figure 13: Ground-based Telemetry Schematic

1. Signal Decoding

The IC demodulator obtained the serial pulse-coded signal from the receiver and separated the signal into the respective seven channels of information. The output on each channel, however, remained in pulse-wave format. This situation required that a prototype electronic circuit be designed to decode each channel's pulse-wave length into an analog DC voltage. Design and testing of this decoder was undertaken by a Postgraduate School Electronics Technician, and a successful circuit design was not available at the time that thesis research was terminated.

Once decoded, the analog signals for channels 1 through 7 were designed for concurrent supply to a cassette data recorder and to a ground station panel arranged with analog meters for direct visual feedback of transmitted data.

2. Ground Station Design

Figure 14 is a schematic of the ground station design. Meters were arranged on the panel to empirically simulate control surface displacements. A 10kΩ potentiometer accompanied each meter for calibration. The lower right corner of the panel was reserved for encoder input calibration using the 15-pin connector previously discussed. Appropriate calibration meters were made selectable via the large rotary knob at the bottom center of the panel.

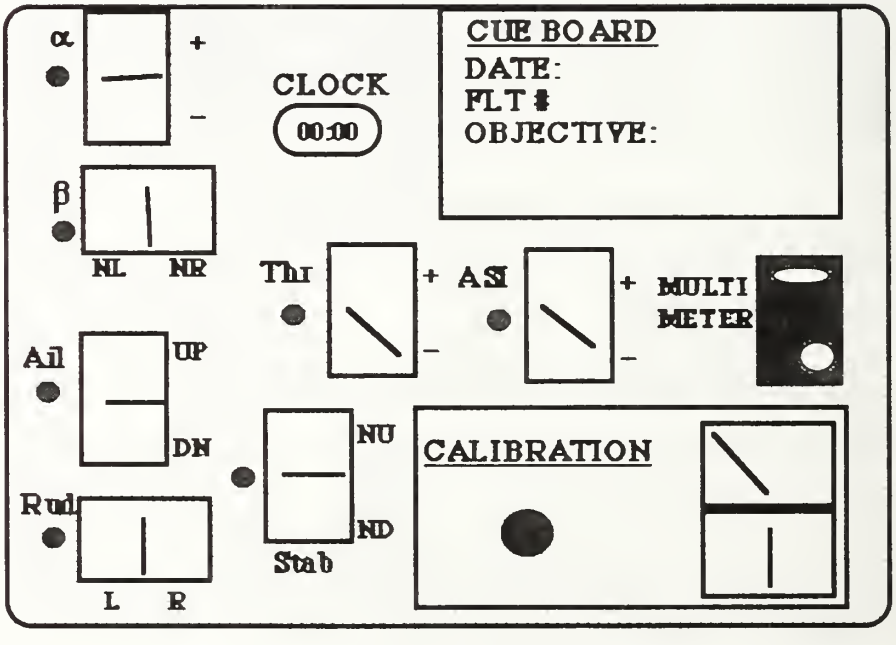

Figure 14: Ground Station Panel Design

Following construction and testing of the ground-based decoder, the analog meters may be calibrated to correspond to airborne encoder inputs. The

ground station could then be videotape recorded during flight tests, with accompanying audio description of the maneuvers being performed. The ground station panel, associated electronics, recorder, and power supply were housed in a portable tool case which simplified transport and set up at the flight test site.

IV. FLIGHT TEST VEHICLE

A. MODEL DESCRIPTION

The 1/8-scale F-16A radio-controlled model was fully assembled and flight tested prior to commencement of the project. The aircraft structure is composed of a pre-formed fiberglass fuselage with high-density foam wings, stabilators, and rudder. It is powered by a Rossi™ 0.90 glow-plug single-piston engine which drives a six-inch diameter, five-bladed, ducted fan. Previous engine thrust tests rated static thrust at 13.5 to14.0 pounds at full power [Ref. 14:pp. 10,13].

Model specifics are as follows:

- Length ..... 73 inches
- Wing Span ..... 48 inches
- Mean Aerodynamic Chord ..... 18.4 inches
- Wing Reference Area ..... 777.6 inches^2
- Aspect Ratio 2.96
- Leading Edge Sweep ..... 40 °
- Taper Ratio 0.218
- Empty Weight (with telemetry & 5 oz. fuel) ..... 13.84 lbs
- Fuel Capacity ..... 24 fl. oz.
- Gross Weight (without counterbalance weights) ..... 14.83 lbs

Figure 15 shows the wing planform of the model. Reference area (S), aspect ratio (AR), taper ratio (λ) and mean aerodynamic chord (MAC) were determined by projecting the line of the leading edge to the centerline and discounting the model strakes. The resulting aspect ratio (2.96) was in agreement with that of the majority of fighter aircraft, which commonly have aspect ratios of about 3.0.

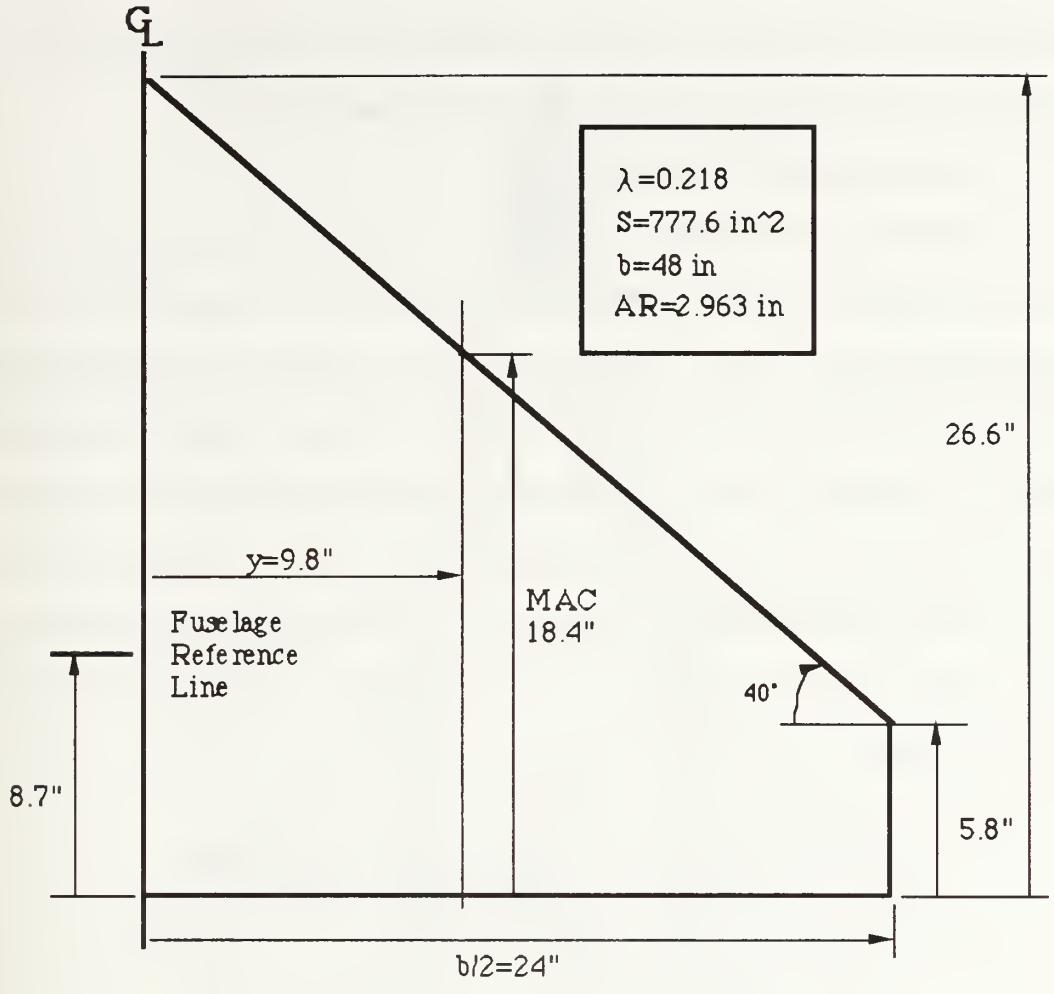

Figure 15: Wing Planform

B. WEIGHT AND BALANCE

A critical requirement of the flight test plan was the ability to precisely determine the model's center-of-gravity (cg) position. It was therefore necessary to be able to weigh and balance the aircraft in the inflight configuration (wheels up) for a variety of cg's ranging from approximately 20% MAC to 30% MAC. A 3/16" wide by 3-1/4" long slot was cut along the upper section of the fuselage centerline which spanned the desired cg range. A 5" long balancing rod with a knife-edged wing nut at its end could then be inserted into the slot to suspend the aircraft for weight and balance measurements. The balancing rod was designed to

be attached to a DC load cell, whose power and output could be accommodated by the portable ground station's power supply and calibration meters.

1. Determining CG Location

On the top of the model fuselage was a cross-sectional groove which was used as a reference line for determining cg locations (Figures 15 and 16). Immediately forward of this reference line, the top surface of the fuselage was parallel to what could be considered the model's waterline. A light-weight plastic bubble level was placed on this surface, and the balancing rod adjusted to a position along the slot until the bubble was centered in the level. The distance from the reference line to the center of the balancing rod was then measured to determine cg position. Table 1 shows cg positions as a percentage of MAC and respective reference distances.

% MAC	Reference distance (in.)
30.0	4.18
29.0	4.36
28.0	4.55
27.0	4.73
26.0	4.92
25.0	5.10
24.0	5.28
23.0	5.47
22.3	**5.60**
22.0	5.65
21.0	5.84
20.0	6.02

TABLE 1: CG Location / Reference Distances
(22.3% MAC is empty weight cg position)

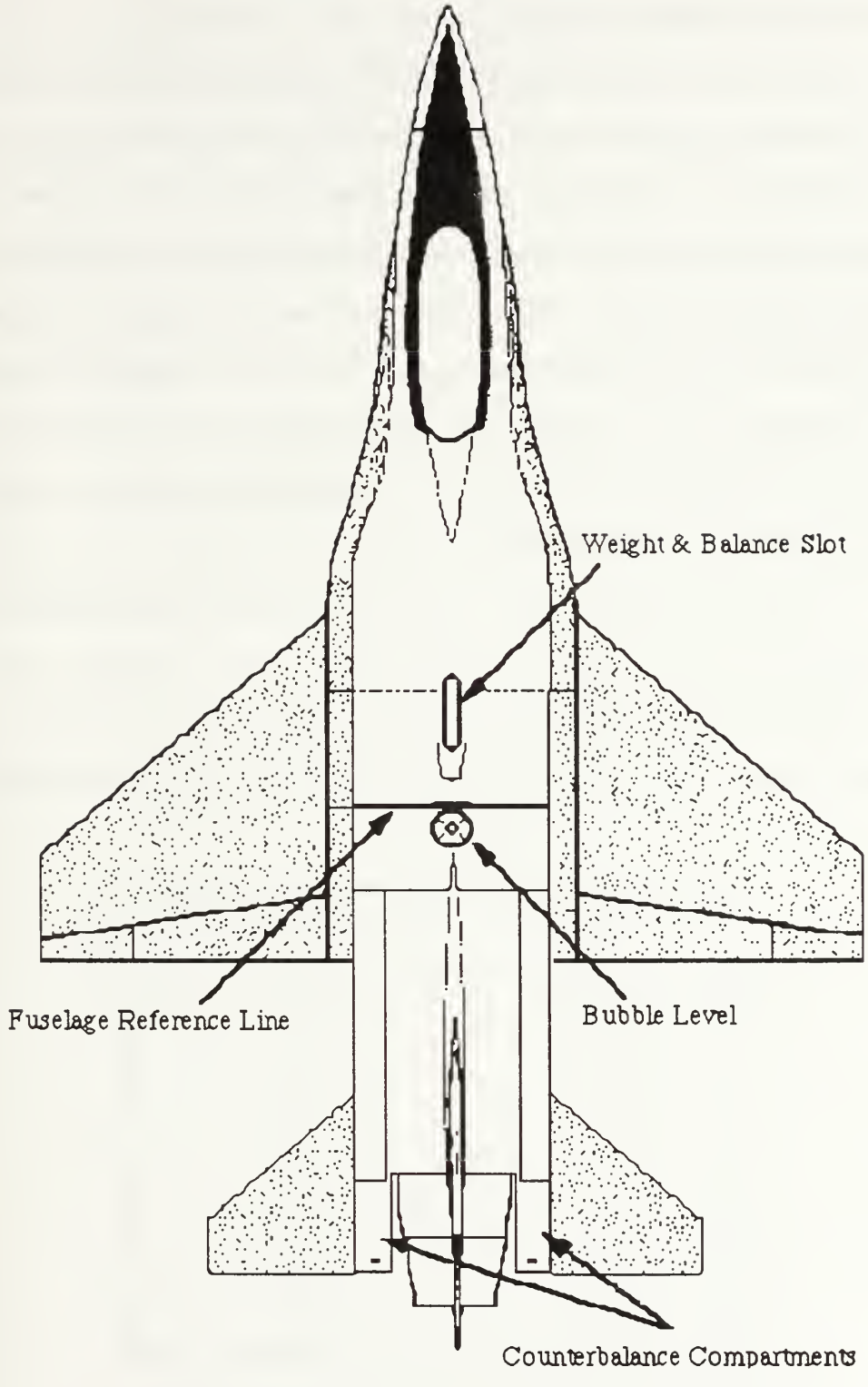

Figure 16: Weight and Balance Modifications

2. Fuel Considerations

The location of the model's fuel cell significantly affected cg position. The 24 fl. oz. fuel cell was located immediately forward of the engine along the fuselage centerline. Its midpoint was 11-1/4 inches forward of the reference line. As a result, fuel consumption during flight is anticipated to have a significant effect on flight behavior. During initial weight and balance testing, the cg position varied from 22.3% MAC at empty weight (5 fl. oz. fuel) to 20.2% MAC at gross weight (24 fl.oz. fuel). The gross weight configuration is, therefore, at the forward end of the cg test range, and counterbalancing weights are required to obtain cg positions aft of 22.3% MAC.

At the aft end of the model -- 22-1/2 inches aft of the reference line -- two compartments on either side of the nozzle provide adequate space for counterbalancing weights (Figure 16). Table 2 lists the counterbalancing weight required to obtain cg positions with the aircraft in the empty weight condition.

% MAC	Weight Required (lbs)
23.0	0.07
24.0	0.16
25.0	0.25
26.0	0.35
27.0	0.44
28.0	0.54
29.0	0.64
30.0	0.74

TABLE 2: Empty Weight Counterbalance Requirements

As a "rule of thumb," the model's cg position will shift forward 2.0% of MAC when fully fueled. Thus, if a 25.0% MAC cg position is desired, the aircraft should be counterbalanced to a 24.0% MAC position (0.16 lbs according to Table 2) and the desired cg position will be bracketed during the course of the flight test.

The model manufacturer recommends that the cg position be approximately 3-1/2 inches forward of the "former," a veneer plywood frame to which the engine duct is mounted. This recommended position corresponds to approximately 4.6 inches forward of the reference line, or approximately 28% MAC in the empty weight condition. To obtain this recommended cg position during flight when taking off in the gross weight condition, it would be necessary to counterbalance with 0.44 lbs.

V. CALIBRATION RESULTS

Following installation of the airborne telemetry package, the model was calibrated to establish reference voltage ranges for the various inputs to the encoder. The alpha and beta vanes, control surface deflections, and throttle position were bench calibrated at the UAV laboratory by extracting their respective encoder inputs to a multimeter using the 15-pin calibration connector. The encoder output signal was simultaneously viewed on an oscilloscope to ensure that voltage ranges did not exceed pulse-width limitations. The airspeed indicator was calibrated in the NPS Aerolab Low Speed Wind Tunnel as a separate unit, then installed on the model.

A. CALIBRATION PROCESS

For each input except airspeed, the calibration process required adjusting two potentiometers: the potentiometer which sensed the deflection and the trimming potentiometer. In general the sensing potentiometer was set to a selected centerpoint voltage (nominal 2.500 volts DC) and the trimming potentiometer adjusted to provide as wide a range in voltage from centerpoint as possible. Adjustments to the trimming potentiometer, however, affected the centerpoint reading. Calibration was therefore an iterative process and varied depending upon the type of sensing potentiometer used for each input (alpha and beta inputs were from 20kΩ pots; stabilator and aileron, from 5kΩ pots; rudder and throttle, from 10kΩ pots).

B. ALPHA AND BETA VANE CALIBRATION

The alpha potentiometer with pinion attached to its shaft was mated with the transverse aluminum rod and gear to provide +140° and -130° of alpha vane displacement. An empirical zero deflection angle was selected, depressed 4° from the waterline, so that the alpha vanes were parallel with the upper surfaces of the left and right leading edge strakes. At this zero deflection angle, the alpha trimming potentiometer was adjusted until the encoder input centerpoint read 2.500 volts. This provided a range of +1.565 volts from centerpoint for +90° of vane displacement and -0.747 volts from centerpoint for -90° of vane displacement; the increased sensitivity was biased toward the high-α side of vane deflection. Figure 17 shows the alpha vane calibration curve and regression constants. Prior to flight testing, it will be necessary to recalibrate the alpha deflection angle against the actual model angle of attack. This may be accomplished in wind tunnel tests or captive carry tests.

The beta potentiometer shaft was set at an initial centerpoint of 2.500 volts and the beta vane attached so that the zero deflection angle was along the fuselage centerline. After attaching the vane and adjusting the trimming potentiometer, the actual centerpoint reading was 2.460 volts with a range of +0.382 volts from centerpoint for +50° of beta vane displacement (positive yaw) and -0.479 volts from centerpoint for -50° of beta vane displacement (negative yaw). Figure 18 shows the beta vane calibration curve and regression constants. Again, the beta vane will need to be recalibrated in wind tunnel or captive carry tests to verify the actual sideslip angle being measured.

Regression constants for all calibration curves fit the equation:

- **Deflection = M0 + M1*Volts + M2*(Volts)²**

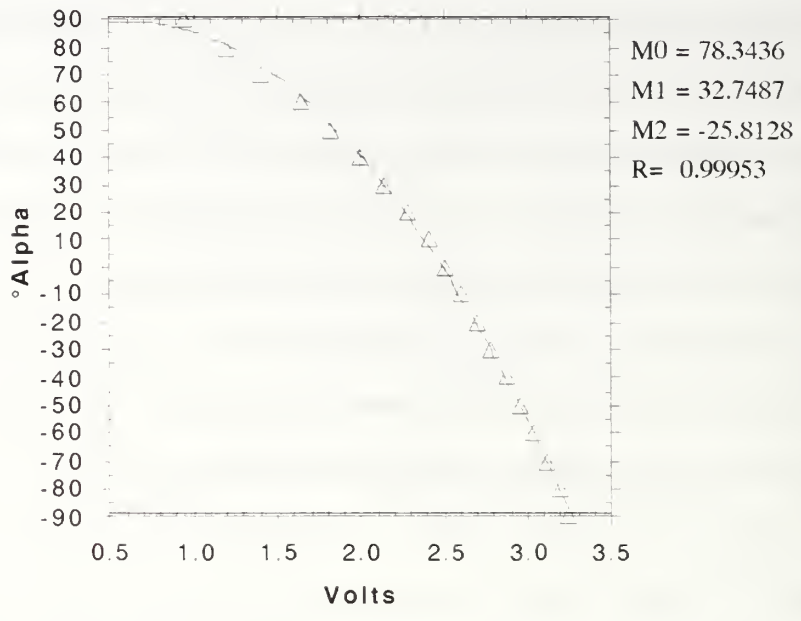

Figure 17: Alpha Vane Calibration Curve

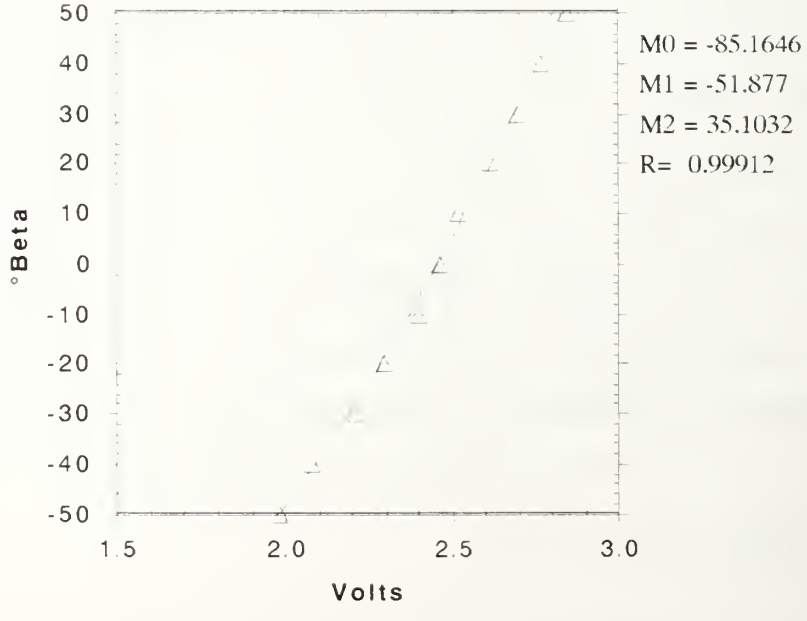

Figure 18: Beta Vane Calibration Curve

C. STABILATOR CALIBRATION

The stabilator zero deflection angle was set such that the trailing edge of the stabilator was parallel with the trailing edge strakes. Perhaps because the stabilator potentiometer was a 5kΩ device, a null setting of 2.500 volts would not provided a sufficient voltage range, and attempts to lower the centerpoint resulted in flooding the channel input to the encoder. A 3.016 centerpoint setting provided a range of -0.336 volts from centerpoint for +7° of stabilator displacement (positive pitch) and +0.265 volts from centerpoint for -6° of stabilator displacement (negative pitch). This was the range of stabilator movement with the radio transmitter elevator down-mixer turned on. (Note: by turning off the elevator down-mixer, the servo/potentiometer mechanical linkage can be exceeded, potentially resulting in binding of the control surface). Figure 19 shows the stabilator calibration curve and regression constants.

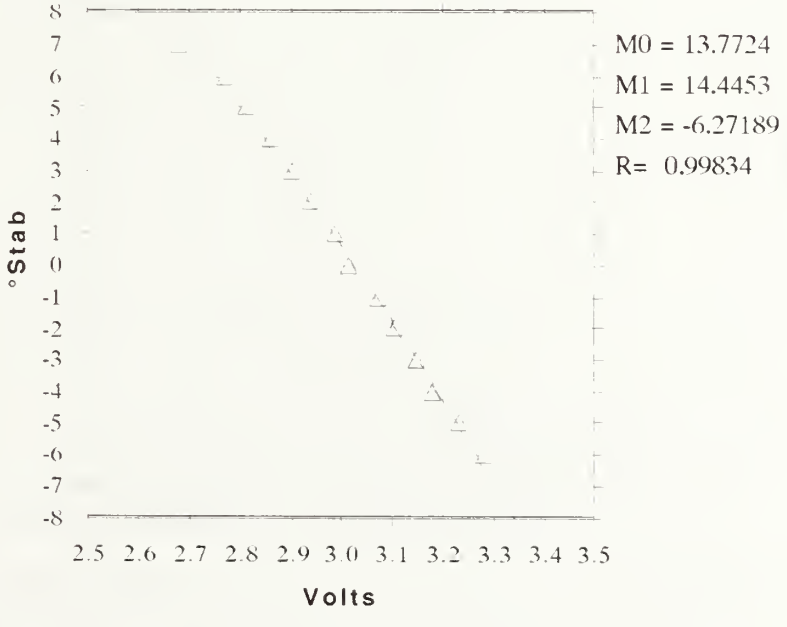

Figure 19: Stabilator Calibration Curve

D. STARBOARD AILERON CALIBRATION

The starboard aileron zero deflection angle was set such that the trailing edge of the aileron was parallel with the wing extension of the strake. The aileron potentiometer was set for a centerpoint reading of 2.905 volts. Again, because this potentiometer was a 5kΩ device, a null setting of 2.500 volts would not have provided a sufficient voltage range for the limited aileron deflection. The 2.905 null setting provided a range of -1.253 volts from centerpoint for 14° of up starboard aileron (positive roll) and +0.837 volts from centerpoint for 18° of down starboard aileron (negative roll). Figure 20 shows the starboard aileron calibration curve and regression constants.

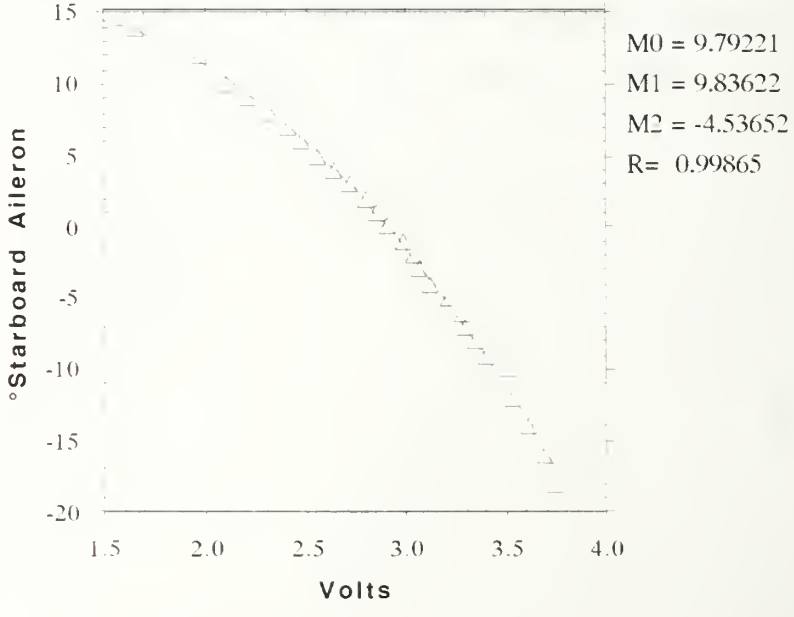

Figure 20: Starboard Aileron Calibration Curve

E. RUDDER CALIBRATION

The rudder zero deflection angle was set such that the trailing edge of the rudder was parallel with the vertical stabilizer. The rudder potentiometer was set for a centerpoint reading of 2.559 volts, and the trimming potentiometer provided a range of -0.484 volts from centerpoint for 12° of right rudder (positive yaw) and +0.396 volts from centerpoint for 12° of left rudder (negative yaw). In the same manner as the stabilator potentiometer signal, the rudder signal sensitivity could not be increased without flooding its respective encoder channel. Figure 21 shows the rudder calibration curve and regression constants.

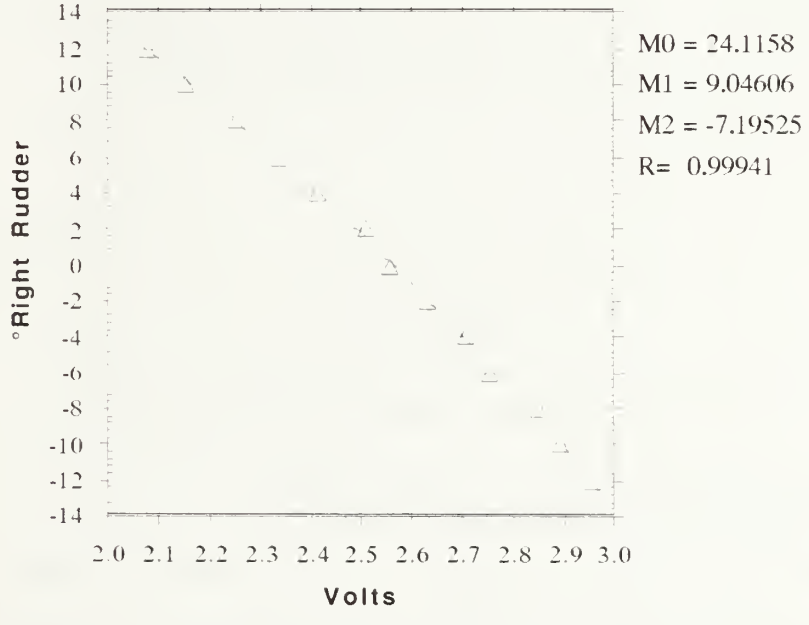

Figure 21: Rudder Calibration Curve

F. THROTTLE POSITION CALIBRATION

Three throttle positions were measured: idle (0%), mid-throttle (centered servo at 50%), and full throttle (100%). Mid-throttle potentiometer output was set

at 2.536 volts and trimmed for a range of +0.608 volts from centerpoint for full throttle, and -0.970 volts from centerpoint for idle. Figure 21 shows the throttle position calibration curve. When the decoder is completed and the ground station calibrated, the throttle position readout on the ground station panel will be further calibrated to provide an indication of fuel consumption rate.

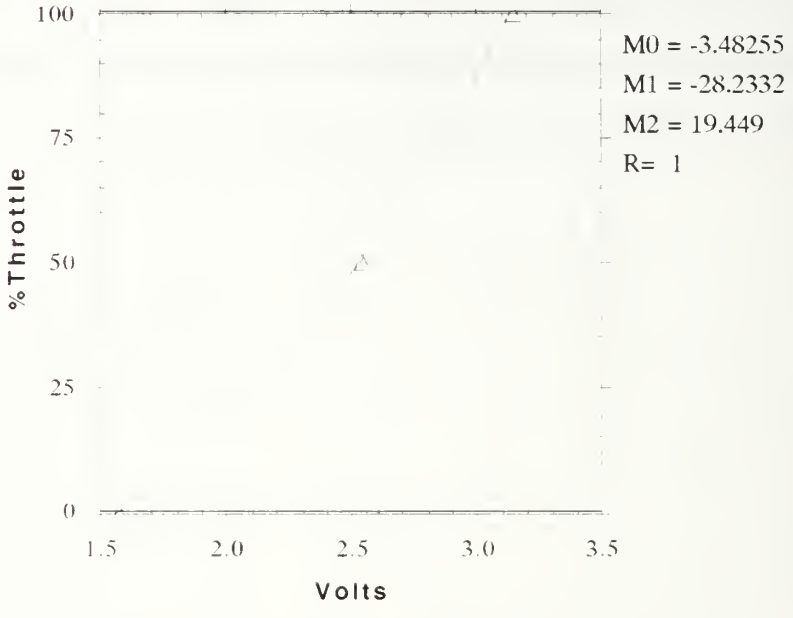

Figure 22: Throttle Position Calibration Curve

G. AIRSPEED INDICATOR CALIBRATION

The airspeed sensor was affixed to a five inch high 90° angled probe and mounted in the NPS Aerolab Low Speed Wind Tunnel for calibration. Sensor leads were routed to the airspeed electronic breadboard outside the tunnel from which output voltages and frequencies were recorded at various tunnel speeds using a multimeter and frequency counter. A total of nine calibration tests were conducted: one with the sensor at 0° deflection to the airstream, and at 5°, 10°, 20°,

and 30° offsets to determine cross-flow effects. Actual wind tunnel airspeed was determined by correlating tunnel Δp (cm H_2O) to q (dynamic pressure). Figure 23 shows the linear relationship between tunnel airstream velocity and the voltage output of the airspeed electronic's frequency-to-voltage conversion. The electronic design provided a very precise and repeatable signal output from 20 mph (below aircraft stall speed) to approximately 110 mph. The slight scatter in the data above 110 mph was attributed to fluctuations in the tunnel airstream which were noted as the tunnel approached its maximum speed. Proposed flight testing, however, will be concentrated on low to medium speed handling characteristics.

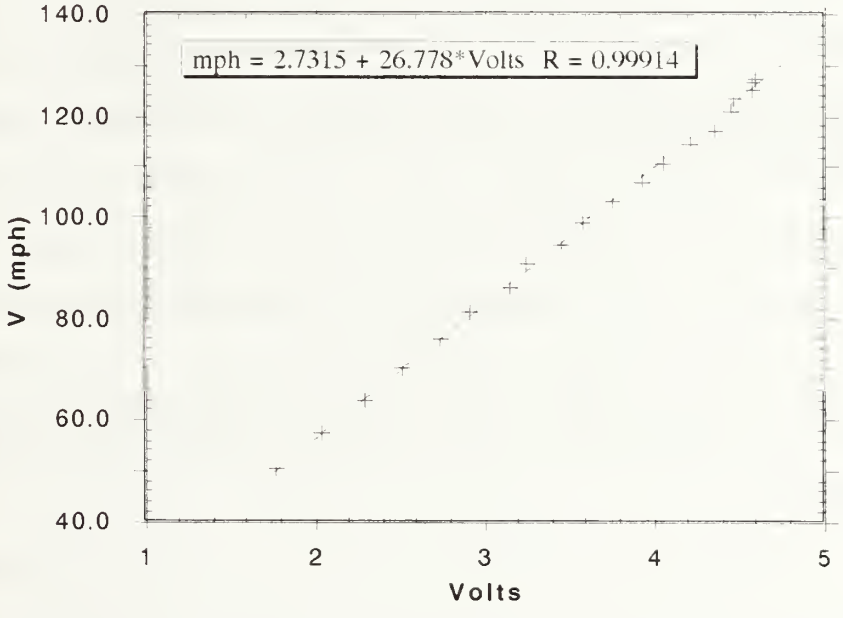

Figure 23: Airspeed Indicator Calibration Curve (0° Offset)

Calibration curves for the 5°, 10°, 20°, and 30° offsets are presented in Appendix A. Several general characteristics were noted in propeller sensor performance from the various offsets:

- As a "rule of thumb," the airspeed sensor read 1 mph less for each degree of offset up to 20°.
- When the sensor was deflected to starboard (airstream approaching from the left), equivalent to right positive yaw or nose-up positive pitch, the maximum airspeed limit was 120 mph. Above 120 mph with starboard offset, the propeller remained at a constant RPM. This characteristic was not noted for port sensor deflections, equivalent to left negative yaw or nose-down negative pitch.

These results showed that it will be necessary to apply pitch and yaw corrections to the transmitted airspeed data. Again, because planned flight tests will concentrate on low to medium flight speeds, the non-linear sensor performance for starboard deflections above 120 mph is not anticipated to be of serious concern.

Following wind tunnel testing, the airspeed sensor was mounted on a 6 inch long boom attached to the top of the vertical stabilizer. The boom was mounted to be parallel with the aircraft's waterline. Prior to actual flight testing, it will be necessary to recalibrate the installed airspeed indicator in wind tunnel or captive carry tests to determine whether disturbed flows or shed vortices from the leading edge strakes interfere with actual airspeed measurement. During these tests, correlations may be made between yaw effects and angle-of-attack effects on airspeed readings.

VI. FLIGHT TEST PROCEDURE

The conduct of flight tests will require a number of procedural steps which are broken down into the categories of flight test preparation, pre-flight checks, proposed flight profile, and post-flight checks.

A. FLIGHT TEST PREPARATION

A day or more before flight testing, a number of items must be prepared to ensure a successful test program:

1. Charge all NiCad batteries:

- Radio Control Transmitter (9.6 VDC, 1200 mAh)
- Control Receiver (4.8 VDC, 500 mAh)
- Airborne Telemetry (9.6 VDC, 1200 mAh)
- Ground Station (9.6 VDC, 1200 mAh)

2. Ensure the following equipment is on hand and in operating condition:

- Radio control transmitter
- Starter toolbox with motorcycle battery
- Starter(s)
- Starter wand and endbolt
- Extra glow plugs
- Glow plug battery
- Model engine fuel
- Retract air pump
- Video camera with cassettes and batteries
- Data recorder with cassettes and batteries
- Hand-held voice recorder with cassettes and batteries
- Voltmeter

- Windspeed indicator
- Tool kit

B. PRE-FLIGHT CHECKS

1. Prior to engine start at the test site, the following steps should be taken:

a. Determine the desired cg position and attach appropriate counterbalance weights;

b. Fuel the aircraft to gross weight condition;

c. Calibrate the load cell with the ground station calibration meter;

d. Suspend the aircraft from the load cell and record weight;

e. Place the bubble level at the reference position and record balanced cg position;

f. Ensure that the airborne telemetry transmitter switch is in the ON position;

g. Ensure that the following hardware is secure:

- Alpha vane and beta vane set screws
- Alpha-beta frame screws
- Stabilator allen bolts
- Wing allen bolts
- Engine bolts
- Throttle socket ball link
- Canopy screws

h. Place the aircraft's radio control receiver switch and telemetry switch to their ON positions (forward);

i. Turn the ground station power supply ON;

j. Perform a verification check of alpha, beta, and control surface deflections against ground station meters.

2. **Following pre-start checks accomplish the following:**

   a. Ensure that the video camera is recording the ground station panel;

   b. Start the ground station recorder and note the tape count on the cue board;

   c. Start and warm up the engine;

   d. Start the ground station clock to track fuel consumption.

C. PROPOSED FLIGHT PROFILE

After takeoff and climb to a test altitude of approximately 300 feet above ground level, a racetrack pattern will be established and the following maneuvers performed:

1. On upwind legs, the aircraft will be trimmed at different airspeeds to determine stabilator control power; and

2. On downwind legs, the aircraft will be will be placed in a slow-speed, high-α attitude and beta sweeps performed to evaluate yaw controllability and rudder power.

In accordance with the test pilot's recommendations, these maneuvers will continue for a flight test period of approximately 4 minutes, which is judged to be a prudent testing time based on fuel consumption rates and on pilot fatigue. During the test maneuvers, the video camera will provide a continuous record of the analog meters and running time, and a continuous commentary of maneuvers and time hacks will be made on the hand-held voice recorder. The aircraft will then be landed and taxied to the test site for shut-down. The ground station clock time will be noted at engine shut-down for later cross-check with fuel consumption rates.

D. POST-FLIGHT CHECKS

After engine shut-down, the aircraft will be weighed and balanced again in the same manner as during pre-flight checks. A record of pre-flight and post-flight weights and cg positions will provide a data base for comparison against the ground station's recorded fuel consumption rates (throttle position vs. engine running time).

After engine shut-down, the ground station and airborne telemetry systems will be turned off to conserve battery power. The ground station recorder will be advanced to the next suitable interval to commence the next flight check.

Following all flight tests, the recorded information will be digitized and appropriate corrections made to the airspeed data to account for alpha and beta deflections.

VII. CONCLUSIONS AND RECOMMENDATIONS

A. SUMMARY AND CONCLUSIONS

The purpose of this project was to develop a telemetry system for transmission of flight-related data from an airborne radio-controlled model to a ground-based receiver and recording station. The telemetry system was designed to be compatible with several scaled flight research aircraft in use at the Naval Postgraduate School UAV Laboratory. The system was specifically designed for use in a 1/8-scale F-16A radio-controlled ducted-fan aircraft that had completed initial flight testing. As was shown in the previous chapters, a successful telemetry design was obtained for the airborne portion of the system. This airborne system included an electronic circuit for conversion of measured airspeed to a voltage output, a means to obtain variable voltage readings from control surface deflections, from throttle position, and from alpha and beta vane deflections, and an electronic encoding and transmitting device.

Three major tests were performed to prepare the F-16A model for flight test with the telemetry installed. These tests included (1) initial calibration in the NPS low-speed wind tunnel of the airspeed sensor and its associated electronics which converted measured sensor vane RPM to a voltage output; (2) calibration of the installed encoding device for voltage inputs from alpha and beta vanes, from rudder, stabilator, and starboard aileron control surface deflections, and for the airspeed voltage input; and (3) weight and balance measurements to establish the cg location with the telemetry package installed, and determine counterbalance requirements for variations in cg as a function of fuel consumption.

A successful RPM to voltage electronics circuit was developed and wind-tunnel tested for the airspeed sensor. The circuit provided a precise signal voltage output from 0 to 4.75 volts DC. The voltage output was completely free of hysterisis and linear from 20 mph to approximately 110 mph. This speed range was well suited to the intended flight regime of the model.

The data encoding device and transmitter were constructed from a combination of in-house and commercially-available components. Inputs to six channels of the encoding device were obtained from potentiometers installed throughout the aircraft to measure surface deflections. These inputs were individually calibrated on a 0--5 VDC scale; however, two of the six calibration curves were marginally acceptable. The stabilator and rudder output voltage swings were less than ±0.5 VDC for full surface deflections. Attempts to increase the voltage output ranges from these potentiometers resulted in flooding of the respective channels to the encoder. The remaining four input signals provided excellent range and signal sensitivity. Output from the encoding device was in the form of a pulse-wave-modulated signal which was monitored during calibration.

A series of weight and balance measurements was made on the F-16A model by suspending it in the wheel-up configuration. After verifying that the model waterline was parallel to the ground using a bubble level, the location of the longitudinal cg was measured from an aircraft reference line and compared to mean aerodynamic chord (MAC). A table of cg locations was derived as a function of onboard fuel. Further weight and balance testing provided a table of counterbalance weights required to obtain specific cg locations. Results indicated that the cg would shift aft approximately 2.0% of MAC as fuel was consumed in

flight. A counterbalancing weight of 0.44 lbs was required to maintain the cg at the manufacturer's recommended location of 28% MAC.

The ground-based portion of the telemetry system was designed and partially constructed; however, the decoding electronics had not been assembled and tested prior to termination of thesis research. Once the decoding electronics have been completed and tested, the F-16A model will be ready for further wind-tunnel calibration and subsequent baseline flight testing.

B. RECOMMENDATIONS

Throughout the course of the research project, a number of recommendations were noted which will either be required prior to flight test or may be beneficial to improve the quality of flight data obtained. They are as follows:

1. The F-16A Aircraft

- Mount the aircraft in the NPS Vertical Wind Tunnel plenum chamber to verify the initial calibration curves for the airspeed indicator and the alpha and beta vanes.
- In the Vertical Wind Tunnel or by captive carry, determine whether shed vortices from the leading edge strakes or separated flow from the wings significantly affect the airspeed sensor as it is presently installed.
- Measure the engine's fuel consumption rate as a function of throttle position. Determine the amount of fuel required (plus a small reserve) for a nominal test flight (approximately 4 minutes).
- Search for or fabricate a conformal fuel tank that fits around the engine and that is closer to the aircraft's recommended cg position. This would reduce inflight cg variations and the need for counterbalancing weights, improving thrust to weight and reducing the likelihood of hard landings.
- Measure the aircraft cg in the inflight (wheels up) configuration.
- Reduce model weight whenever possible.

2. The Airborne Telemetry System

- Verify that the ground plane antenna and data transmission antenna are the proper lengths for the frequency used. This will ensure maximum range, interference-free reception.
- Isolate the airborne telemetry package from engine vibrations with foam rubber. Prolonged high frequency vibrations may damage solder connections and electronic components.
- Continue attempts to recalibrate the stabilator and rudder potentiometer input signals to achieve greater sensitivity to the respective control surface deflections.

3. The Telemetry Ground Station

- Physically ground the electrical system during flight tests using a spike driven into the ground .
- Obtain a load cell suitable for use with the ground station's 9 volt DC battery for weight and balance measurements. A "fish scale" is too inaccurate. A suitable load cell could be quickly calibrated at the test sight with an appropriate calibration weight. Extra meters were included on the calibration section of the ground station panel for this purpose.

APPENDIX A

AIRSPEED INDICATOR ELECTRONICS CALIBRATION DATA

Run #1	0° Orientation					
Baro pres. psi	Tunnel temp °F	Tunnel dens. slug/ft^3	cm H2O	V mph	M-meter volts	M-meter ±volts
29.95	68.0	0.002342	19.97	127.4	4.59	0.05
29.95	70.0	0.002333	19.26	125.4	4.58	0.08
29.95	71.0	0.002328	17.80	120.7	4.45	0.06
29.95	72.0	0.002324	16.75	117.2	4.35	0.06
29.95	73.0	0.002320	15.96	114.5	4.22	0.05
29.95	73.0	0.002320	14.91	110.6	4.05	0.04
29.95	74.0	0.002315	13.88	106.8	3.93	0.04
29.95	74.0	0.002315	12.92	103.1	3.75	0.05
29.95	74.0	0.002315	11.90	98.9	3.58	0.04
29.95	74.0	0.002315	10.97	95.0	3.45	0.05
29.95	74.0	0.002315	10.05	90.9	3.25	0.05
29.95	74.0	0.002315	9.06	86.3	3.15	0.04
29.95	74.0	0.002315	8.04	81.3	2.91	0.04
29.95	74.0	0.002315	7.01	75.9	2.74	0.03
29.95	74.0	0.002315	6.01	70.3	2.51	0.04
29.95	74.0	0.002315	4.95	63.8	2.29	0.03
29.95	74.0	0.002315	4.02	57.5	2.04	0.03
29.95	74.0	0.002315	3.06	50.2	1.77	0.02
29.95	75.0	0.002311	18.50	123.5	4.46	0.05
29.95	76.0	0.002307	19.50	126.9	4.57	0.03

Run #2	10° Stbd	rd Orientation				
Baro pres. psi	Tunnel temp °F	Tunnel dens. slug/ft^3	cm H2O	V mph	M-meter volts	M-meter ±volts
29.95	75.0	0.002311	20.56	130.2	4.09	0.01
29.95	75.0	0.002311	19.64	127.2	4.07	0.01
29.95	76.0	0.002307	18.50	123.6	4.04	0.02
29.95	77.0	0.002302	17.56	120.5	4.00	0.03
29.95	78.0	0.002298	16.50	116.9	3.91	0.03
29.95	78.0	0.002298	15.51	113.4	3.78	0.03
29.95	78.0	0.002298	14.50	109.6	3.65	0.03
29.95	78.0	0.002298	13.51	105.8	3.51	0.03
29.95	78.0	0.002298	12.33	101.1	3.34	0.06
29.95	78.0	0.002298	11.20	96.3	3.23	0.04
29.95	78.0	0.002298	10.10	91.5	3.04	0.05
29.95	78.0	0.002298	9.01	86.4	2.87	0.06
29.95	78.0	0.002298	6.29	72.2	2.40	0.04
29.95	78.0	0.002298	5.10	65.0	2.14	0.04
29.95	78.0	0.002298	3.57	54.4	1.79	0.03
29.95	78.0	0.002298	11.93	99.4	3.32	0.04
29.95	78.0	0.002298	14.02	107.8	3.57	0.04
29.95	78.0	0.002298	12.85	103.2	3.43	0.04

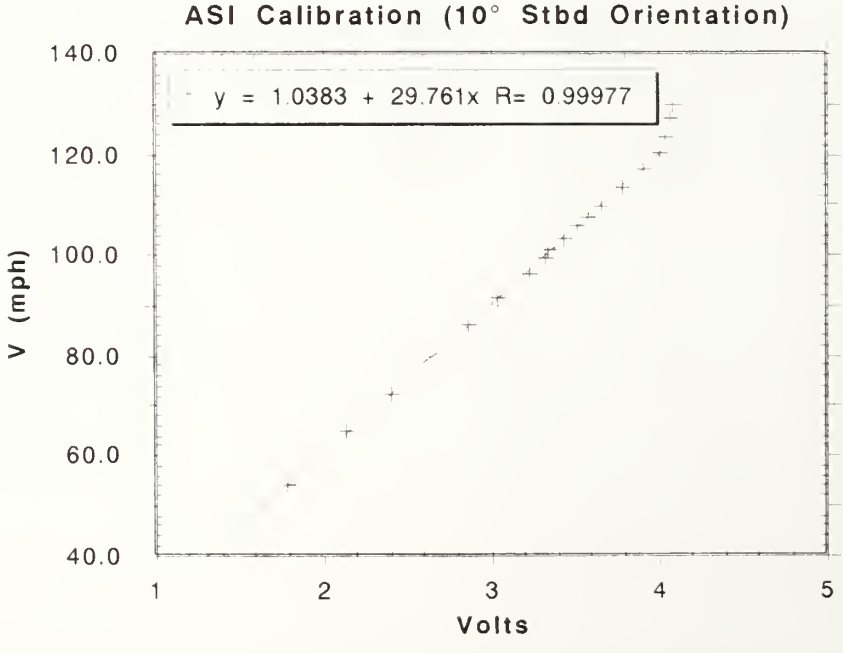

Run #3	20° Stbd					
Baro pres. psi	Tunnel temp °F	Tunnel dens. slug/ft^3	cm H2O	V mph	M-meter volts	M-meter ±volts
29.95	77.0	0.002302	20.17	129.2	3.62	0.02
29.95	78.0	0.002298	18.78	124.8	3.58	0.03
29.95	78.0	0.002298	17.15	119.2	3.47	0.03
29.95	79.0	0.002294	15.85	114.7	3.32	0.03
29.95	79.0	0.002294	14.52	109.8	3.18	0.03
29.95	79.0	0.002294	13.24	104.8	3.03	0.03
29.95	79.0	0.002294	12.17	100.5	2.92	0.05
29.95	79.0	0.002294	11.05	95.8	2.80	0.04
29.95	79.0	0.002294	9.76	90.0	2.62	0.04
29.95	79.0	0.002294	8.28	82.9	2.38	0.04
29.95	79.0	0.002294	6.67	74.4	2.14	0.04
29.95	79.0	0.002294	5.47	67.4	1.95	0.03
29.95	79.0	0.002294	4.24	59.3	1.70	0.03
29.95	79.0	0.002294	2.14	42.2	1.22	0.02

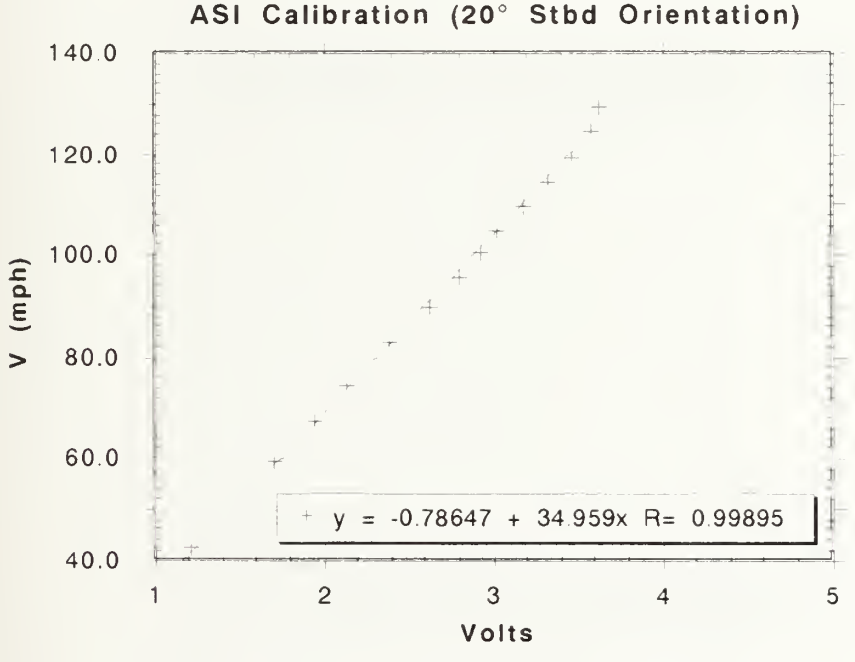

Run #4	30° Stbd					
Baro pres. psi	Tunnel temp °F	Tunnel dens. slug/ft^3	cm H2O	V mph	M-meter volts	M-meter ±volts
29.95	78.0	0.002298	20.39	130.0	3.30	0.02
29.95	79.0	0.002294	19.26	126.5	3.30	0.02
29.95	80.0	0.002289	18.05	122.5	3.29	0.01
29.95	80.0	0.002289	17.23	119.7	3.28	0.01
29.95	81.0	0.002285	15.97	115.4	3.19	0.02
29.95	81.0	0.002285	14.88	111.4	3.09	0.03
29.95	81.0	0.002285	13.48	106.0	2.98	0.03
29.95	81.0	0.002285	12.10	100.4	2.84	0.03
29.95	81.0	0.002285	11.16	96.4	2.74	0.03
29.95	81.0	0.002285	9.77	90.2	2.56	0.03
29.95	81.0	0.002285	8.33	83.3	2.38	0.03
29.95	81.0	0.002285	7.15	77.2	2.13	0.02
29.95	81.0	0.002285	6.62	74.3	2.03	0.02
29.95	81.0	0.002285	4.80	63.2	1.67	0.02
29.95	80.0	0.002289	2.88	48.9	1.35	0.02
29.95	80.0	0.002289	1.75	38.2	1.02	0.02

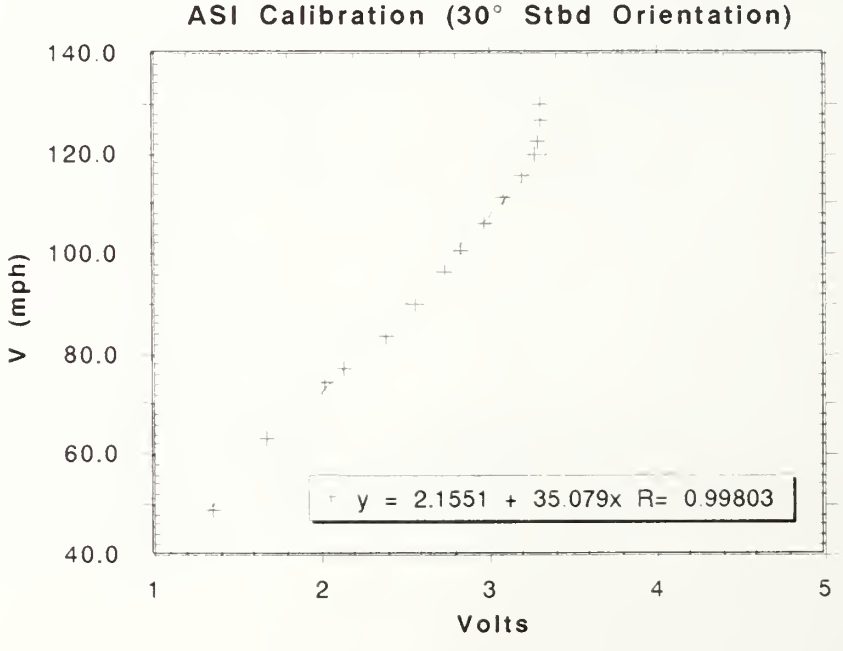

Run #5	5° Stbd					
Baro pres. psi	Tunnel temp °F	Tunnel dens. slug/ft^3	cm H2O	V mph	M-meter volts	M-meter ±volts
29.95	81.0	0.002285	19.78	128.4	4.12	0.01
29.95	82.0	0.002281	20.66	131.3	4.12	0.01
29.95	83.0	0.002277	18.89	125.7	4.13	0.01
29.95	83.0	0.002277	17.46	120.8	4.05	0.05
29.95	84.0	0.002273	16.40	117.2	3.98	0.03
29.95	84.0	0.002273	15.25	113.0	3.81	0.04
29.95	84.0	0.002273	14.00	108.3	3.67	0.04
29.95	84.0	0.002273	12.58	102.7	3.48	0.04
29.95	84.0	0.002273	11.13	96.6	3.26	0.04
29.95	83.0	0.002277	9.60	89.6	3.04	0.06
29.95	83.0	0.002277	8.15	82.6	2.79	0.03
29.95	83.0	0.002277	6.75	75.1	2.55	0.03
29.95	83.0	0.002277	5.52	67.9	2.31	0.04
29.95	83.0	0.002277	4.26	59.7	2.00	0.03
29.95	82.0	0.002281	3.08	50.7	1.68	0.03
29.95	82.0	0.002281	1.46	34.9	1.12	0.01

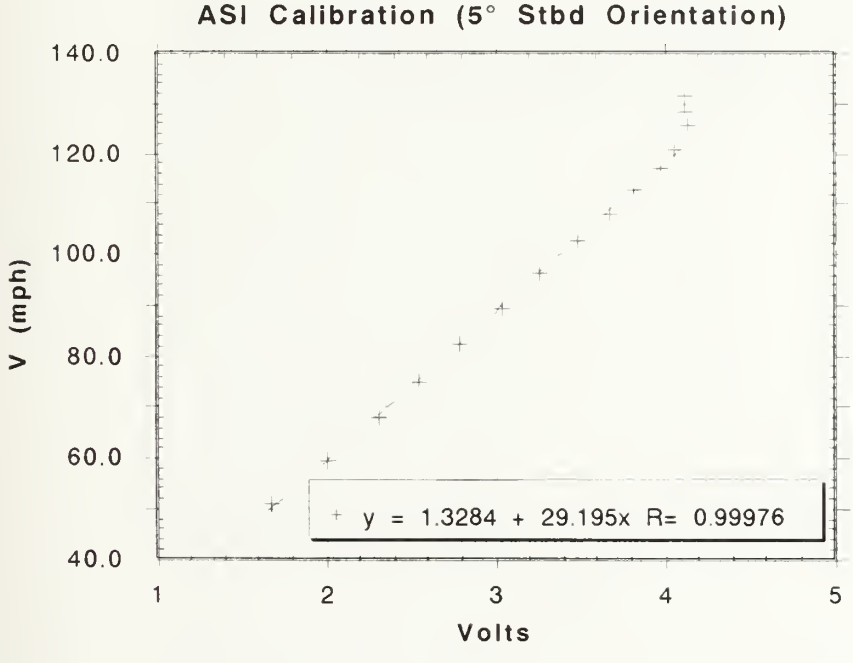

Run #6	5° Port					
Baro pres. psi	Tunnel temp °F	Tunnel dens. slug/ft^3	cm H2O	V mph	M-meter volts	M-meter ±volts
29.95	82.0	0.002281	20.94	132.2	4.54	0.04
29.95	83.0	0.002277	19.76	128.6	4.41	0.06
29.95	83.0	0.002277	18.27	123.6	4.23	0.04
29.95	83.0	0.002277	16.96	119.1	4.11	0.06
29.95	84.0	0.002273	15.55	114.1	3.90	0.04
29.95	84.0	0.002273	13.85	107.7	3.68	0.04
29.95	84.0	0.002273	12.10	100.7	3.46	0.03
29.95	84.0	0.002273	10.86	95.4	3.27	0.04
29.95	84.0	0.002273	9.50	89.2	3.05	0.04
29.95	83.0	0.002277	8.00	81.8	2.80	0.03
29.95	83.0	0.002277	6.62	74.4	2.54	0.04
29.95	83.0	0.002277	5.22	66.1	2.24	0.03
29.95	83.0	0.002277	4.02	58.0	1.93	0.02
29.95	82.0	0.002281	2.76	48.0	1.59	0.02
29.95	82.0	0.002281	1.40	34.2	1.13	0.02

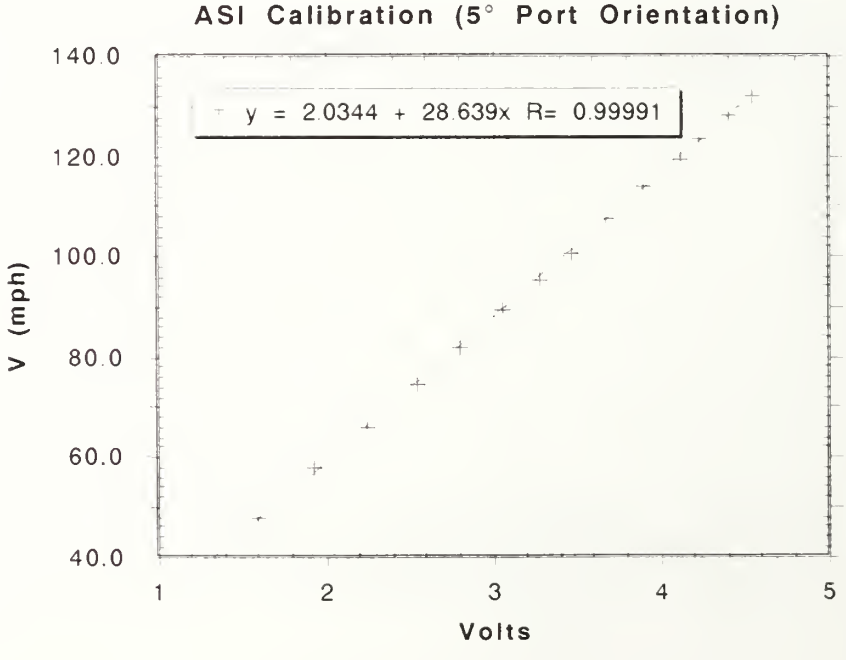

Run #7	10° Port					
Baro pres. psi	Tunnel temp °F	Tunnel dens. slug/ft^3	cm H2O	V mph	M-meter volts	M-meter ±volts
29.95	83.0	0.002277	20.25	130.1	4.10	0.05
29.95	84.0	0.002273	19.13	126.6	4.02	0.04
29.95	84.0	0.002273	17.75	122.0	3.88	0.06
29.95	84.0	0.002273	16.10	116.1	3.69	0.03
29.95	84.0	0.002273	14.68	110.9	3.56	0.04
29.95	84.0	0.002273	13.38	105.9	3.38	0.03
29.95	84.0	0.002273	12.04	100.4	3.19	0.02
29.95	84.0	0.002273	10.75	94.9	3.02	0.03
29.95	84.0	0.002273	9.30	88.3	2.79	0.04
29.95	84.0	0.002273	8.03	82.0	2.61	0.03
29.95	84.0	0.002273	6.75	75.2	2.38	0.03
29.95	84.0	0.002273	5.50	67.9	2.16	0.03
29.95	84.0	0.002273	4.25	59.7	1.85	0.03
29.95	84.0	0.002273	3.00	50.1	1.57	0.03
29.95	84.0	0.002273	2.18	42.7	1.32	0.01
29.95	83.0	0.002277	1.08	30.1	0.90	0.02

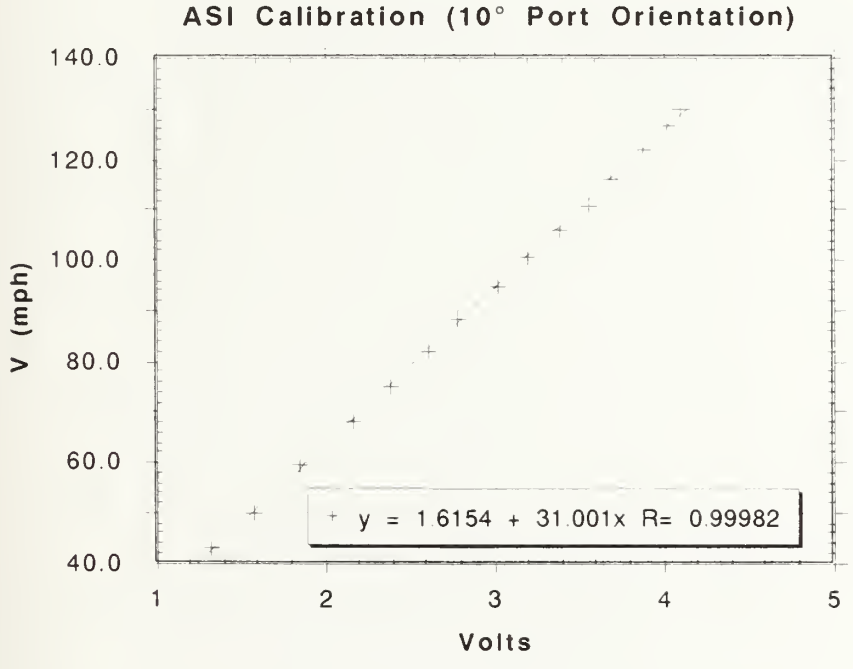

Run #8	20° Port					
Baro pres. psi	Tunnel temp °F	Tunnel dens. slug/ft^3	cm H2O	V mph	M-meter volts	M-meter ±volts
29.95	83.0	0.002277	20.30	130.3	3.72	0.03
29.95	84.0	0.002273	19.10	126.5	3.61	0.04
29.95	84.0	0.002273	17.75	122.0	3.51	0.03
29.95	84.0	0.002273	16.45	117.4	3.37	0.04
29.95	84.0	0.002273	15.25	113.0	3.27	0.04
29.95	84.0	0.002273	14.02	108.4	3.14	0.04
29.95	84.0	0.002273	12.76	103.4	2.97	0.03
29.95	84.0	0.002273	11.50	98.2	2.72	0.03
29.95	84.0	0.002273	10.25	92.7	2.66	0.03
29.95	84.0	0.002273	9.00	86.8	2.48	0.03
29.95	84.0	0.002273	7.75	80.6	2.33	0.03
29.95	84.0	0.002273	6.50	73.8	2.10	0.02
29.95	84.0	0.002273	5.25	66.3	1.86	0.04
29.95	83.0	0.002277	4.01	57.9	1.61	0.02
29.95	83.0	0.002277	2.62	46.8	1.33	0.03
29.95	83.0	0.002277	1.52	35.7	1.00	0.01

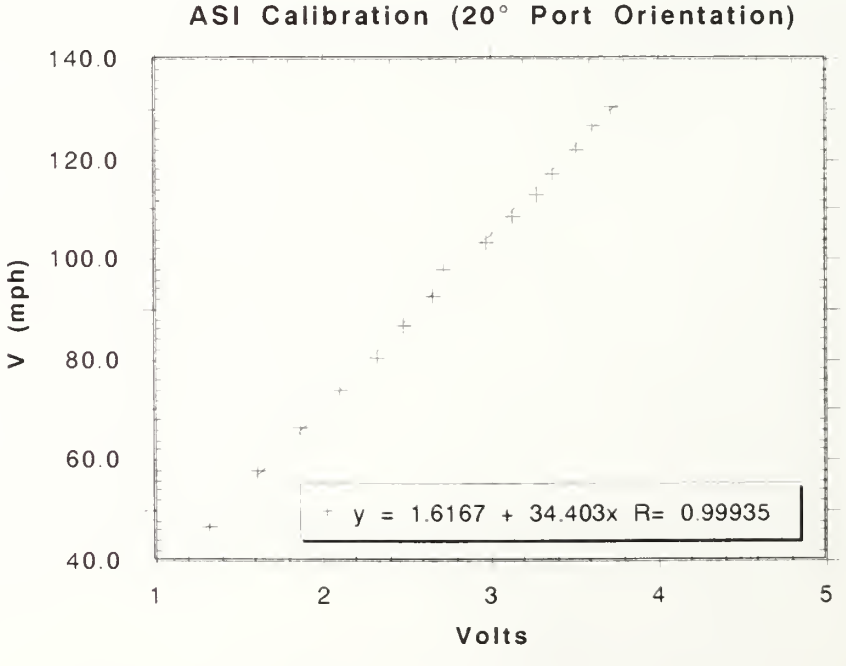

Run #9	30° Port					
Baro pres. psi	Tunnel temp °F	Tunnel dens. slug/ft^3	cm H2O	V mph	M-meter volts	M-meter ±volts
29.95	84.0	0.002273	20.61	131.4	4.11	0.03
29.95	84.0	0.002273	19.25	127.0	4.00	0.04
29.95	84.0	0.002273	18.00	122.8	3.78	0.03
29.95	84.0	0.002273	16.75	118.5	3.69	0.02
29.95	84.0	0.002273	15.50	114.0	3.57	0.02
29.95	84.0	0.002273	14.25	109.3	3.43	0.04
29.95	84.0	0.002273	13.00	104.4	3.29	0.03
29.95	84.0	0.002273	11.75	99.2	3.13	0.02
29.95	84.0	0.002273	10.50	93.8	2.94	0.03
29.95	84.0	0.002273	9.25	88.0	2.76	0.03
29.95	84.0	0.002273	8.00	81.9	2.55	0.03
29.95	84.0	0.002273	6.75	75.2	2.33	0.03
29.95	84.0	0.002273	5.50	67.9	2.09	0.03
29.95	84.0	0.002273	4.25	59.7	1.76	0.02
29.95	84.0	0.002273	3.00	50.1	1.46	0.01
29.95	84.0	0.002273	1.75	38.3	1.14	0.01
29.95	83.0	0.002277	0.85	26.7	0.77	0.01

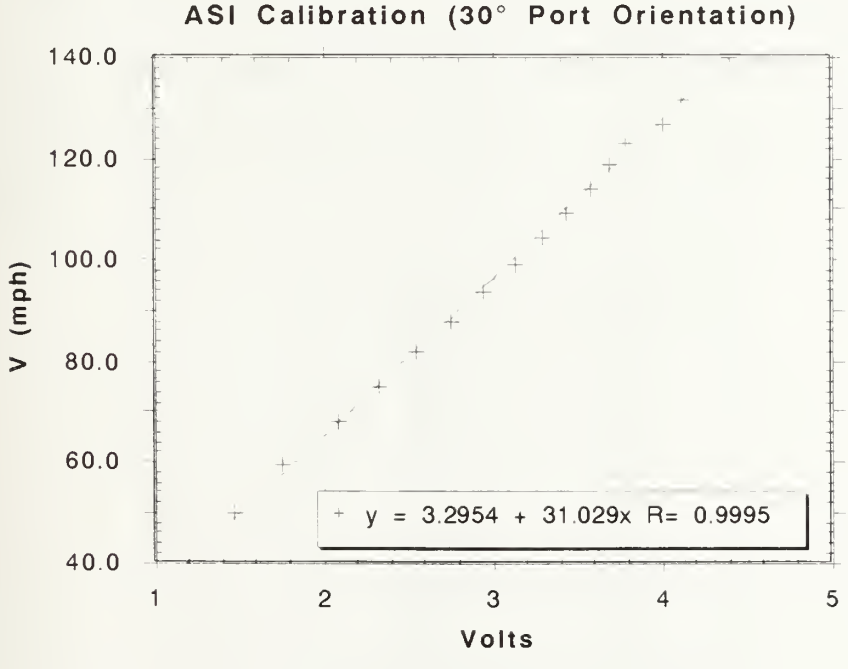

APPENDIX B

AIRBORNE TELEMETRY/POTENTIOMETER CALIBRATION DATA

The following data was obtained by measuring the voltage input signals from the various deflection potentiometers to the airborne encoder.

A. ALPHA VANE CALIBRATION

Zero degrees alpha was defined as 4° above the waterline such that the vanes are parallel with the top of the leading edge strakes. Positive alpha is nose up, vane tip down; negative alpha is nose down, vane tip up. Centerpoint voltage was adjusted to 2.500 VDC prior to calibration. Alpha was input to Channel 1 on the encoder.

° Alpha	Volts
90	0.935
80	1.201
70	1.412
60	1.642
50	1.827
40	2.002
30	2.144
20	2.277
10	2.405
0	2.500
-10	2.600
-20	2.704
-30	2.785
-40	2.874
-50	2.956
-60	3.028
-70	3.110
-80	3.190
-90	3.247

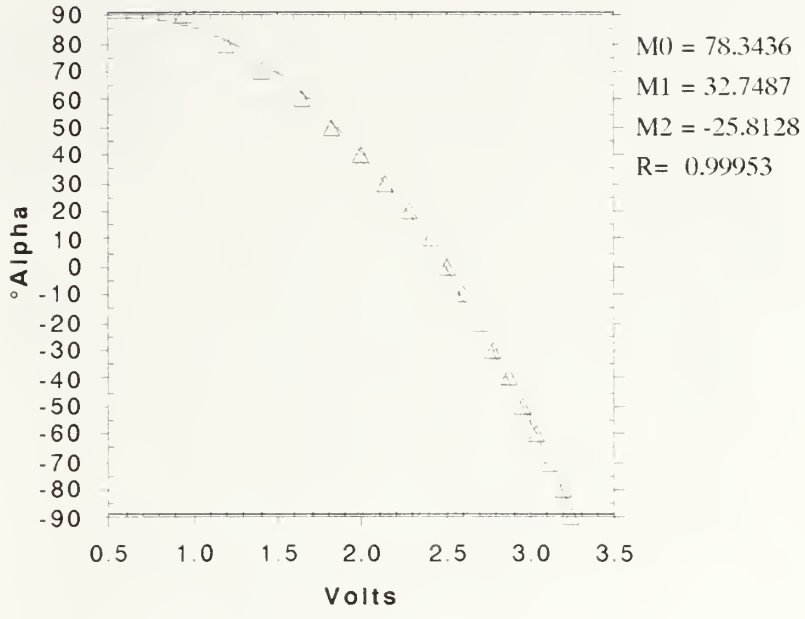

B. BETA VANE CALIBRATION

Zero degrees beta was defined with the beta vane parallel to the longitudinal axis. Positive beta is nose right, vane tip left; negative beta is nose left, vane tip right. Centerpoint voltage was adjusted to 2.500 VDC prior,but was remeasured at 2.460 VDC after the vane was attached. Beta was input to Channel 2 on the encoder.

° Beta	Volts
50	1.981
40	2.077
30	2.211
20	2.298
10	2.395
0	2.460
-10	2.522
-20	2.615
-30	2.692
-40	2.769
-50	2.842

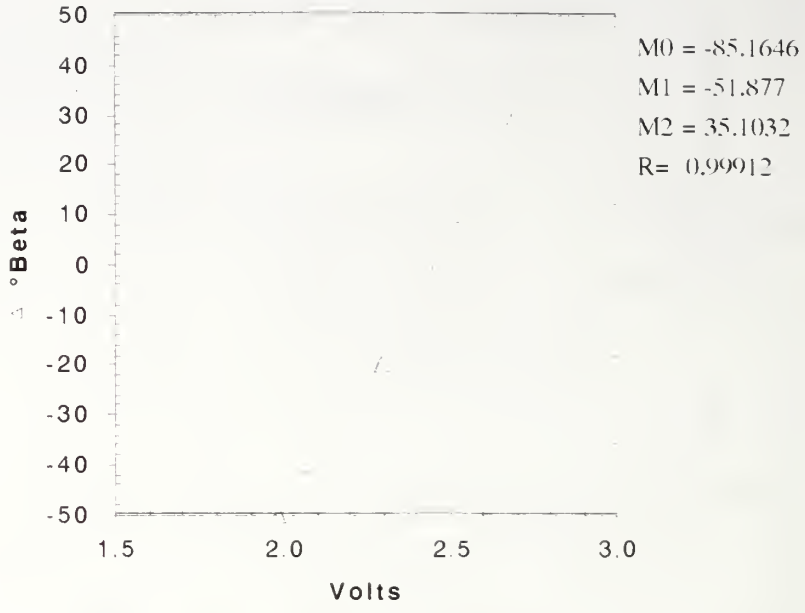

C. STABILATOR CALIBRATION

Zero degrees "stab" (i.e., stabilator) was defined with the trailing edge of the stabilators coincident to the aft fuselage strakes. Positive stab pitches the nose up; negative stab pitches the nose down. Centerpoint voltage was adjusted to 3.016 VDC. Stab was input to Channel 3 on the encoder.

° Stab	Volts
7	2.680
6	2.767
5	2.813
4	2.860
3	2.905
2	2.941
1	2.987
0	3.016
-1	3.071
-2	3.103
-3	3.146
-4	3.180
-5	3.232
-6	3.218

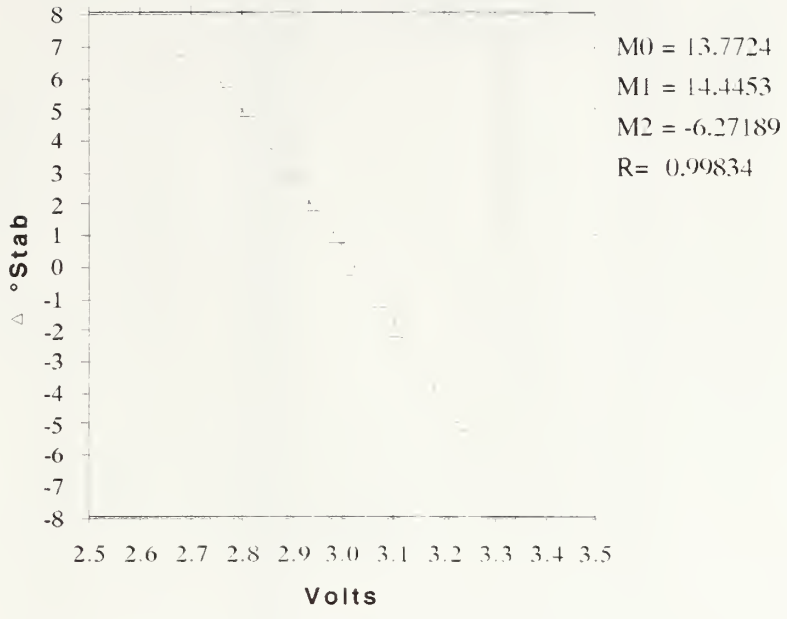

D. STARBOARD AILERON CALIBRATION

Zero degrees starboard aileron was defined with the trailing edge of the aileron parallel with the wing strake. Positive (up) aileron produces positive roll; negative (down) aileron produces negative roll. Centerpoint voltage was adjusted to 2.905 VDC . Starboard aileron was input to Channel 4 on the encoder.

° Aileron Down	Volts
18	3.742
16	3.684
14	3.612
12	3.535
10	3.507
9	3.392
8	3.347
7	3.295
6	3.273
5	3.208
4	3.120
3	3.060
2	3.032
1	2.985
0	2.905
-1	2.858
-2	2.792
-3	2.717
-4	2.642
-5	2.556
-6	2.484
-7	2.408
-8	2.316
-9	2.219
-10	2.110
-12	1.974
-14	1.652

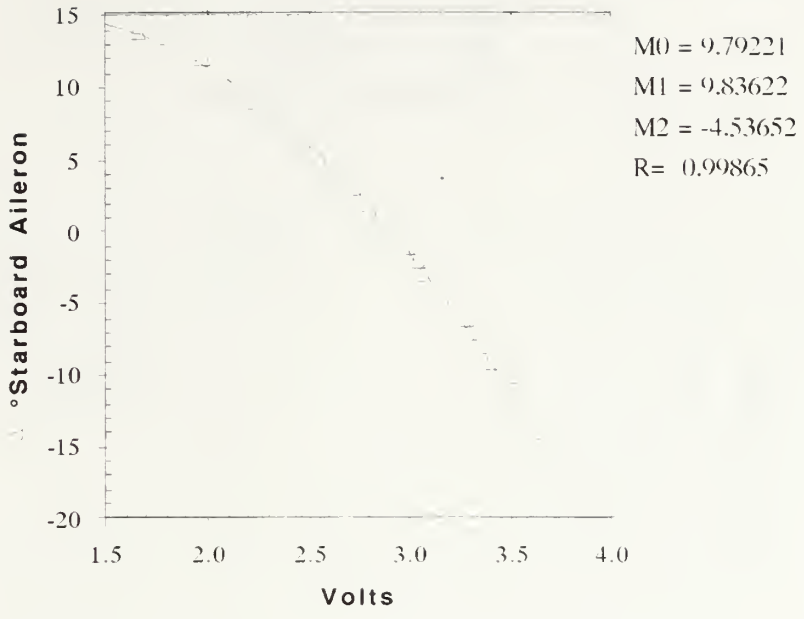

E. RUDDER CALIBRATION

Zero degrees rudder was defined with the trailing edge of the rudder centered with the vertical stabilizer. Positive (right) rudder produces positive yaw; negative (left) rudder produces negative yaw. This sign convention differs from other standards, but is in accordance with the Air Force sign convention. Centerpoint voltage was adjusted to 2.559 VDC . Rudder was input to Channel 6 on the encoder.

°Right Rudder	Volts
12	2.075
10	2.155
8	2.251
6	2.340
4	2.412
2	2.507
0	2.559
-2	2.632
-4	2.705
-6	2.751

-8	2.849
-10	2.891
-12	2.955

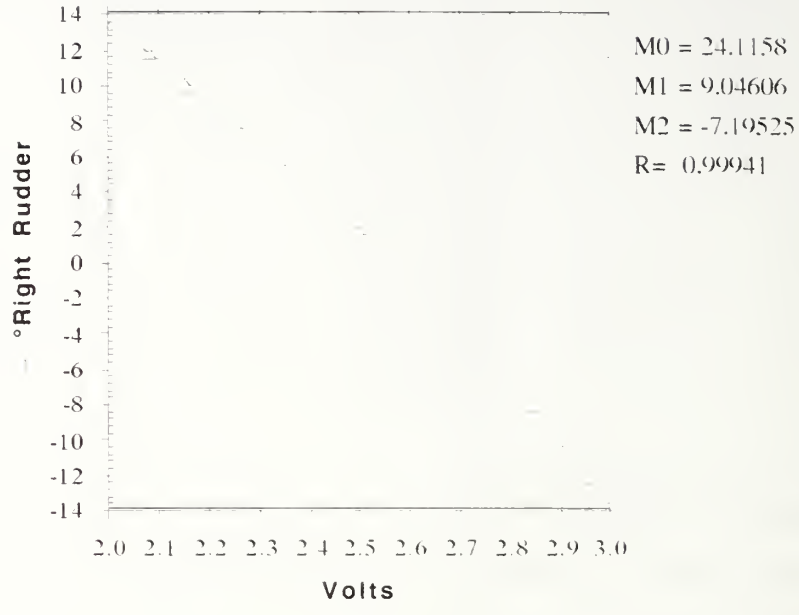

F. THROTTLE POSITION CALIBRATION

Null throttle was set with the radio-control transmitter turned off to allow the throttle servo to seek its zero load position. Two other readings were taken: full throttle and idle with the radio-control transmitter turned on to set these servo positions. Centerpoint voltage was adjusted to 2.536 VDC . Throttle was input to Channel 5 on the encoder.

% Throttle	Volts
0	1.566
50	2.536
100	3.144

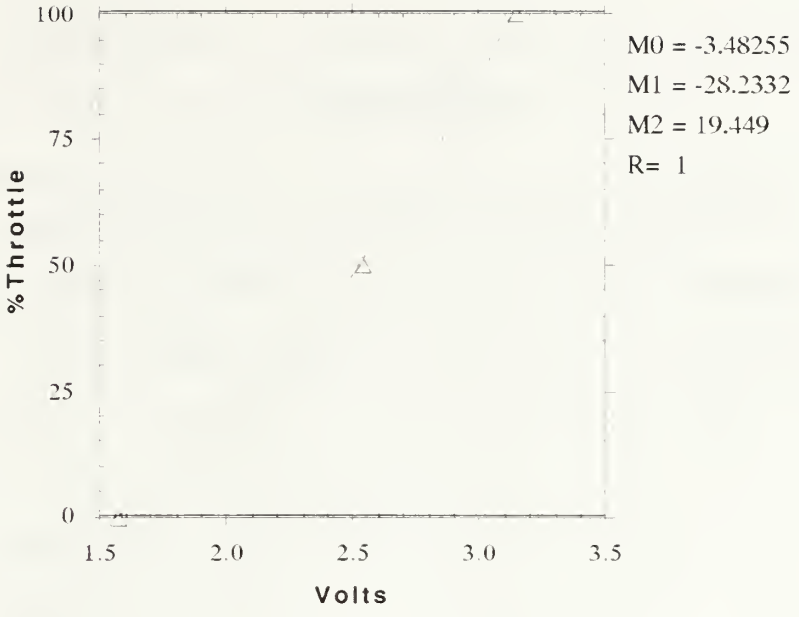
100
75
50
25
0
% Throttle
1.5
2.0
2.5
3.0
3.5
Volts
M0 = -3.48255
M1 = -28.2332
M2 = 19.449
R= 1

APPENDIX C

WEIGHT AND BALANCE CALCULATIONS

1. Determine %MAC as function of Reference Distance on exterior fuselage. Determine the Empty Weight MAC.

The fuselage reference line (Figures 15 & 16) is 8.70 inches forward of the trailing edge of the wing. The weight and balance slot on top of the fuselage extends from 3.50 inches forward of the reference line to 6.75 inches forward of the reference line. Column A increments this distance by 0.25 inches. The bold 5.6 figure is the reference distance for the cg at empty weight. Column B adds the slot distance to the reference line distance from the wing trailing edge to obtain the total distance from the wing trailing edge. Column C subtracts Column B from the mean aerodynamic chord (MAC). MAC = 18.4 inches (Figure 15). Column D

Reference Line = 8.70			
A	B	C	D
Inches fwd of ref	A + ref	18.4 - B	% MAC
3.50	12.20	6.20	33.70
3.75	12.45	5.95	32.34
4.00	12.70	5.70	30.98
4.25	12.95	5.45	29.62
4.50	13.20	5.20	28.26
4.75	13.45	4.95	26.90
5.00	13.70	4.70	25.54
5.25	13.95	4.45	24.18
5.50	14.20	4.20	22.83
5.60	**14.30**	**4.10**	**22.28**
5.75	14.45	3.95	21.47
6.00	14.70	3.70	20.11
6.25	14.95	3.45	18.75
6.50	15.20	3.20	17.39
6.75	15.45	2.95	16.03

expresses the reference distance as a percentage of MAC. The empty weight MAC is located at 22.3% MAC. TABLE 1 was derived from this data.

2. Determine the effect of fuel addition on the location of the cg. (See the computer formulae on the following pages.)

The fuel tank holds 24 fl. oz. of model aviation fuel. The tank is capable of holding 32 fl. oz., but when tipped on its side inside the aircraft it will fill to 24 fl. oz. maximum. The tank midpoint is located 11.25 inches forward of the fuselage reference line. The empty weight of the aircraft (all instrumentation, batteries, engine and fuel tank with 5 fl. oz. of unusable fuel included) is 13.84 lbs.

With the fuel tank full to 32 fl. oz. it weighed 1.824 lbs on the electronic scale. When empty at 5 fl. oz. it weighed 0.420 lbs. Taking the difference and dividing by the difference in fuel (27 fl. oz.), the fuel weighs 0.052 lb/fl.oz.

Column I increments useable fuel from 5 to 24 fl. oz. Column J computes the empty weight moment from the fuselage reference line. Column K calculates the additional moment about the reference line for the fuel tank with fuel. Column M computes the model total weight as fuel is added. Column N determines the reference distance to cg. Column O adds 8.7 inches to the reference distance to determine the distance from the trailing edge of the wing. Column P computes the percent MAC of the cg as the fuel is added.

To hold the cg at 25%MAC the cg reference distance must stay at 5.1 inches. Columns R and S calculate the counterbalance weights required to be placed in two compartments (Figure 16) 22-1/2 inches aft of the fuselage reference line, to hold the cg at 25%MAC. From Cell R5, a 0.25 lb counterweight is required to move the cg position aft to 25%MAC from the 22.3%MAC empty weight condition with no counterweight. TABLE 2 is derived from similar calculations.

	I	J	K	L	M
1	**Wt/Bal with Fuel Co**				
2	Empty wt fuel defined as				
3	Fuel tank location		11.25		
4	fl.oz. fuel	empty mmt	fuel +mmt	total mmt	total wt
5	5	=13.84*5.6	=(I5-5)*0.052*11.25	=J5+K5	=13.84+(I5-5)*0.052
6	=I5+1	=13.84*5.6	=(I6-5)*0.052*11.25	=J6+K6	=13.84+(I6-5)*0.052
7	=I6+1	=13.84*5.6	=(I7-5)*0.052*11.25	=J7+K7	=13.84+(I7-5)*0.052
8	=I7+1	=13.84*5.6	=(I8-5)*0.052*11.25	=J8+K8	=13.84+(I8-5)*0.052
9	=I8+1	=13.84*5.6	=(I9-5)*0.052*11.25	=J9+K9	=13.84+(I9-5)*0.052
10	=I9+1	=13.84*5.6	=(I10-5)*0.052*11.25	=J10+K10	=13.84+(I10-5)*0.052
11	=I10+1	=13.84*5.6	=(I11-5)*0.052*11.25	=J11+K11	=13.84+(I11-5)*0.052
12	=I11+1	=13.84*5.6	=(I12-5)*0.052*11.25	=J12+K12	=13.84+(I12-5)*0.052
13	=I12+1	=13.84*5.6	=(I13-5)*0.052*11.25	=J13+K13	=13.84+(I13-5)*0.052
14	=I13+1	=13.84*5.6	=(I14-5)*0.052*11.25	=J14+K14	=13.84+(I14-5)*0.052
15	=I14+1	=13.84*5.6	=(I15-5)*0.052*11.25	=J15+K15	=13.84+(I15-5)*0.052
16	=I15+1	=13.84*5.6	=(I16-5)*0.052*11.25	=J16+K16	=13.84+(I16-5)*0.052
17	=I16+1	=13.84*5.6	=(I17-5)*0.052*11.25	=J17+K17	=13.84+(I17-5)*0.052
18	=I17+1	=13.84*5.6	=(I18-5)*0.052*11.25	=J18+K18	=13.84+(I18-5)*0.052
19	=I18+1	=13.84*5.6	=(I19-5)*0.052*11.25	=J19+K19	=13.84+(I19-5)*0.052
20	=I19+1	=13.84*5.6	=(I20-5)*0.052*11.25	=J20+K20	=13.84+(I20-5)*0.052
21	=I20+1	=13.84*5.6	=(I21-5)*0.052*11.25	=J21+K21	=13.84+(I21-5)*0.052
22	=I21+1	=13.84*5.6	=(I22-5)*0.052*11.25	=J22+K22	=13.84+(I22-5)*0.052
23	=I22+1	=13.84*5.6	=(I23-5)*0.052*11.25	=J23+K23	=13.84+(I23-5)*0.052
24	=I23+1	=13.84*5.6	=(I24-5)*0.052*11.25	=J24+K24	=13.84+(I24-5)*0.052

	N	O	P	R	S
1					
2				Wt to adjust balance	
3				to 25% MAC	
4	ref distance		% MAC	lbs	oz
5	=L5/M5	=8.7+N5	=(18.4-O5)/18.4*100	=(L5-5.1*M5)/27.6	=R5*16
6	=L6/M6	=8.7+N6	=(18.4-O6)/18.4*100	=(L6-5.1*M6)/27.6	=R6*16
7	=L7/M7	=8.7+N7	=(18.4-O7)/18.4*100	=(L7-5.1*M7)/27.6	=R7*16
8	=L8/M8	=8.7+N8	=(18.4-O8)/18.4*100	=(L8-5.1*M8)/27.6	=R8*16
9	=L9/M9	=8.7+N9	=(18.4-O9)/18.4*100	=(L9-5.1*M9)/27.6	=R9*16
10	=L10/M10	=8.7+N10	=(18.4-O10)/18.4*100	=(L10-5.1*M10)/27.6	=R10*16
11	=L11/M11	=8.7+N11	=(18.4-O11)/18.4*100	=(L11-5.1*M11)/27.6	=R11*16
12	=L12/M12	=8.7+N12	=(18.4-O12)/18.4*100	=(L12-5.1*M12)/27.6	=R12*16
13	=L13/M13	=8.7+N13	=(18.4-O13)/18.4*100	=(L13-5.1*M13)/27.6	=R13*16
14	=L14/M14	=8.7+N14	=(18.4-O14)/18.4*100	=(L14-5.1*M14)/27.6	=R14*16
15	=L15/M15	=8.7+N15	=(18.4-O15)/18.4*100	=(L15-5.1*M15)/27.6	=R15*16
16	=L16/M16	=8.7+N16	=(18.4-O16)/18.4*100	=(L16-5.1*M16)/27.6	=R16*16
17	=L17/M17	=8.7+N17	=(18.4-O17)/18.4*100	=(L17-5.1*M17)/27.6	=R17*16
18	=L18/M18	=8.7+N18	=(18.4-O18)/18.4*100	=(L18-5.1*M18)/27.6	=R18*16
19	=L19/M19	=8.7+N19	=(18.4-O19)/18.4*100	=(L19-5.1*M19)/27.6	=R19*16
20	=L20/M20	=8.7+N20	=(18.4-O20)/18.4*100	=(L20-5.1*M20)/27.6	=R20*16
21	=L21/M21	=8.7+N21	=(18.4-O21)/18.4*100	=(L21-5.1*M21)/27.6	=R21*16
22	=L22/M22	=8.7+N22	=(18.4-O22)/18.4*100	=(L22-5.1*M22)/27.6	=R22*16
23	=L23/M23	=8.7+N23	=(18.4-O23)/18.4*100	=(L23-5.1*M23)/27.6	=R23*16
24	=L24/M24	=8.7+N24	=(18.4-O24)/18.4*100	=(L24-5.1*M24)/27.6	=R24*16

	I	J	K	L	M	N	O	P	R	S
1	**Wt/Bal with Fuel Considerations**									
2	Empty wt fuel defined as 5 oz.								Wt to adjust balance	
3	Fuel tank location		11.25						to 25% MAC	
4	fl.oz. fuel	empty mmt	fuel +mmt	total mmt	total wt	ref distance		% MAC	lbs	oz
5	5	77.50	0.00	77.50	13.84	5.60	14.30	22.28	0.251	4.0
6	6	77.50	0.59	78.09	13.89	5.62	14.32	22.17	0.262	4.2
7	7	77.50	1.17	78.67	13.94	5.64	14.34	22.05	0.274	4.4
8	8	77.50	1.76	79.26	14.00	5.66	14.36	21.94	0.285	4.6
9	9	77.50	2.34	79.84	14.05	5.68	14.38	21.83	0.297	4.8
10	10	77.50	2.93	80.43	14.10	5.70	14.40	21.72	0.309	4.9
11	11	77.50	3.51	81.01	14.15	5.72	14.42	21.61	0.320	5.1
12	12	77.50	4.10	81.60	14.20	5.74	14.44	21.50	0.332	5.3
13	13	77.50	4.68	82.18	14.26	5.76	14.46	21.39	0.343	5.5
14	14	77.50	5.27	82.77	14.31	5.78	14.48	21.28	0.355	5.7
15	15	77.50	5.85	83.35	14.36	5.80	14.50	21.17	0.367	5.9
16	16	77.50	6.44	83.94	14.41	5.82	14.52	21.06	0.378	6.1
17	17	77.50	7.02	84.52	14.46	5.84	14.54	20.96	0.390	6.2
18	18	77.50	7.61	85.11	14.52	5.86	14.56	20.85	0.401	6.4
19	19	77.50	8.19	85.69	14.57	5.88	14.58	20.75	0.413	6.6
20	20	77.50	8.78	86.28	14.62	5.90	14.60	20.64	0.425	6.8
21	21	77.50	9.36	86.86	14.67	5.92	14.62	20.54	0.436	7.0
22	22	77.50	9.95	87.45	14.72	5.94	14.64	20.44	0.448	7.2
23	23	77.50	10.53	88.03	14.78	5.96	14.66	20.34	0.459	7.3
24	24	77.50	11.12	88.62	14.83	5.98	14.68	20.24	0.471	7.5

APPENDIX D

ELECTRONICS AND WIRING DIAGRAMS

The following information is primarily a review of the details of the telemetry design:

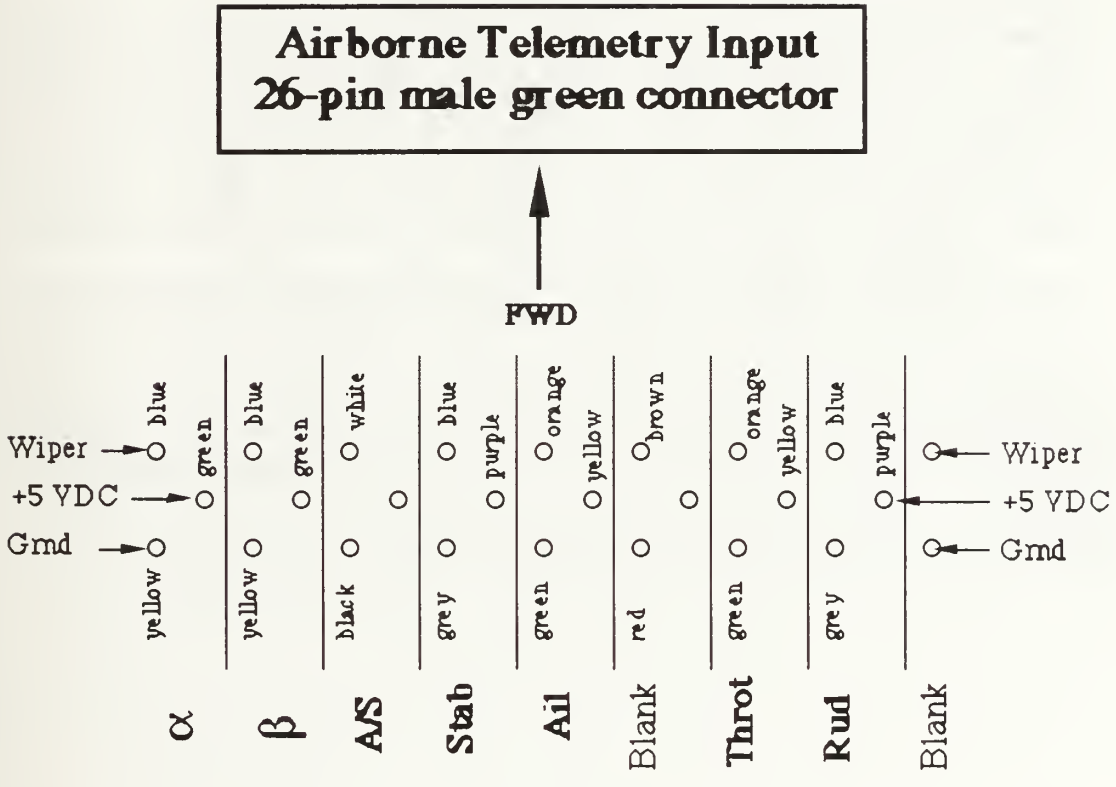

- This is the view of the 26-pin green male connector in the model with wire color code for the wires that come from the various potentiometers.
- The alpha and beta bundles have the same color codes, but the three pin connectors at the end of each bundle are reversed (male/female) so that alpha won't get plugged into the beta potentiometer and vice versa.
- All pins along the bottom row go to a common ground.

- All pins in the middle row are supplied from the encoder's +5 Volt DC Reference Source.
- All pins along the top row are the wiper (or drain) returns from the potentiometers.
- Note that those pins without color assignments or without labels were not used (left blank). The Stab and Aileron 5kΩ potentiometers had an extra post for measuring the centerpoint of the pot. Comparing this post's output to the drain and obtaining a null reading would indicate that the pot was centered. This feature was not used, so there are extra pins available on the connector for future use.
- The airspeed black and white wires go back to the vertical stab and up to the airspeed sensor's green and white leads. There is no voltage supplied to this sensor. Refer to Tom Christian's airspeed circuit diagram to see where these wires attach to the circuit. The wiring for the sensor has been taken care of on the telemetry circuit board, and it makes no difference whether the sensor is connected green-black/white-white or green-white/white-black. All the airspeed circuit sees is an increase in resistance as the photo sensor is blocked.
- There should be no confusion on how this input plug attaches to the telemetry circuit board. The telemetry package is installed with the transmitter forward toward the nose of the aircraft (the transmitter side is the one with the protective cover that has all the holes drilled in it for some of the larger parts that stick out). The green input connector has male and female clamping screws that are on alternate sides of the connector. When attaching the connector to the telemetry package, carefully alternate screwing down one side then the other side so that the pins don't get bent.

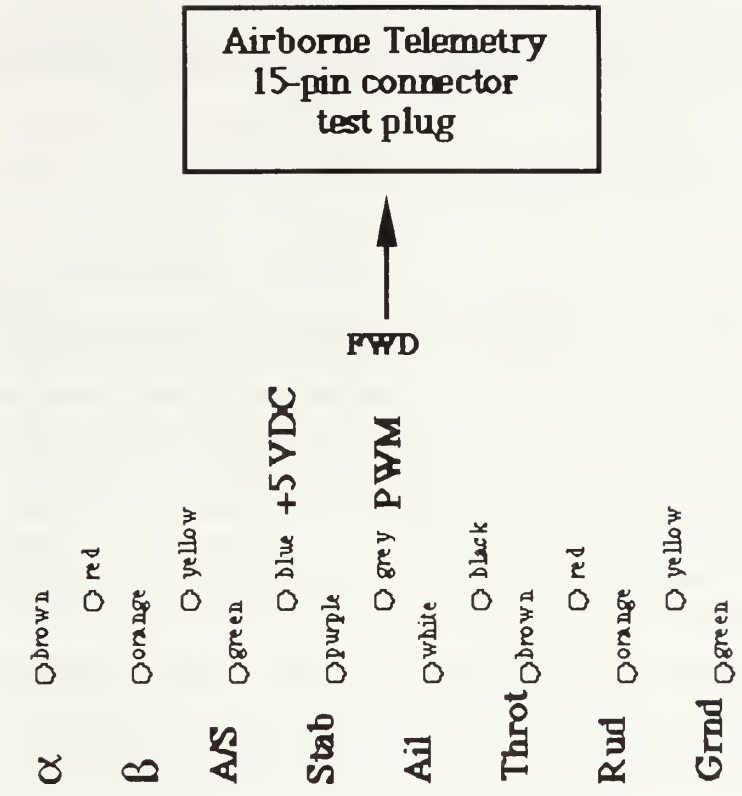

- The 15-pin connector is provided on the airborne telemetry package for sampling the potentiometer and airspeed inputs before they go to the encoder.
- They are arranged in the same way (alpha, beta, A/S, Stab, etc.) as the 26 pin connector, but they don't go to the encoder in this order. It was decided that because the airspeed input wasn't powered from the encoder's 5 Volt Reference Supply, that the airspeed input would go to the last channel, as follows:

  Channel 1 - Alpha

  Channel 2 - Beta

  Channel 3 - Stab

  Channel 4 - Aileron

  Channel 5 - Throttle

  Channel 6 - Rudder

  Channel 7 - Airspeed

- Again, those colored wires that don't have labels are left blank.
- Perhaps a timing gun (like those used to set the timing/RPM on a car) placed in

front of the photo sensor at a frequency within the range of the airspeed circuit, could be used to check the voltage output of the airspeed circuit. (Frequency/voltage conversion plot follows).

- The ground and +5 VDC are common to the encoder's references so that the ref voltage can also be easily checked.
- The PWM grey wire comes from the encoder output, so this can be sampled and sent to the oscilloscope to view the PWM signal during calibration. It is very important when calibrating the aircraft that the encoder signal be monitored. It is possible to get a range spread from centerpoint for a given reading (e.g., alpha or beta) that reads out on the multimeter, but this range may exceed the limits of the pulse wave for that channel when viewed on the oscilloscope. The beta input is a good example: by rotating the beta vane ± 50° a wide voltage swing appears on the multimeter and the beta channel expands and contracts on the oscilloscope; however, when exceeding ±50°, the voltage will continue to swing on the multimeter, but the oscilloscope reaches a limit and chops off the signal.
- There is a trimming potentiometer on the telemetry circuitboard for the airspeed input. Once the airspeed circuit has been calibrated in the wind tunnel this potentiometer should be removed or at least never touched. Adjusting it will completely nullify any calibration efforts. It's the one on the end (marked 10K A/S). The output from the LM2917 airspeed circuit is the green wire that's threaded through the board and over to that trim pot. It should be rewired directly to channel 7 on the 5044 chip, which is the red wire that is presently hanging loose.
- The TX on/off switch on the board supplies 9.6 Volt power to the transmitter. When ready for flight test, this switch should be turned on. It was installed to check the encoder inputs and output during calibration without draining the battery or smoke-checking the transmitter.
- With reference to the plugboard layout, the "component side" of the TM circuitboard is the side with the encoder and trimming pots. From left to right the gold contacts are:

  1) ground

  2) + side of airspeed sensor

  3) +5 volt reference from encoder

  4) +5 volt reference from encoder

  5) airspeed voltage output from the airspeed circuit. This output goes to the encoder channel 7 and also to this contact and then to the 15-pin connector to test the airspeed voltage.

  6) ground

7) PWM signal from the encoder. This goes to the transmitter and also to the 15-pin connector to test the PWM signal.

8) +5 volt reference from encoder

9) +5 volt reference from encoder

10) 9.6 volt power for the transmitter

11) ground

12) 9.6 volt power for the encoder and the airspeed circuit

13) +5 volt reference from encoder

14) +5 volt reference from encoder

15) alpha potentiometer wiper input - goes to the alpha trim pot & channel 1

16) ground

17) beta potentiometer wiper input - goes to the beta trim pot & channel 2

18) stab pot wiper input - goes to the stab trim pot & channel 3

19) aileron pot wiper input - goes to the aileron trim pot & channel 4

20) throttle pot wiper input - goes to the throttle trim pot & channel 5

21) ground

22) rudder pot wiper input - goes to the rudder trim pot & channel 6

- If the transmitter or encoder is removed from the circuitboard, be careful to note that there are small washers attached as spacers to ensure that the solder points on these circuits don't contact the solder points on the circuitboard.
- The three-pin connectors for the 9.6 Volt battery supply should be replaced with new connectors. Ensure that all switches are turned off and that positive (red) battery goes to positive (red) supply for the TM when the battery is connected. All TM connections use the square 3-pin connectors and all radio connections use the flat "banana" connectors.

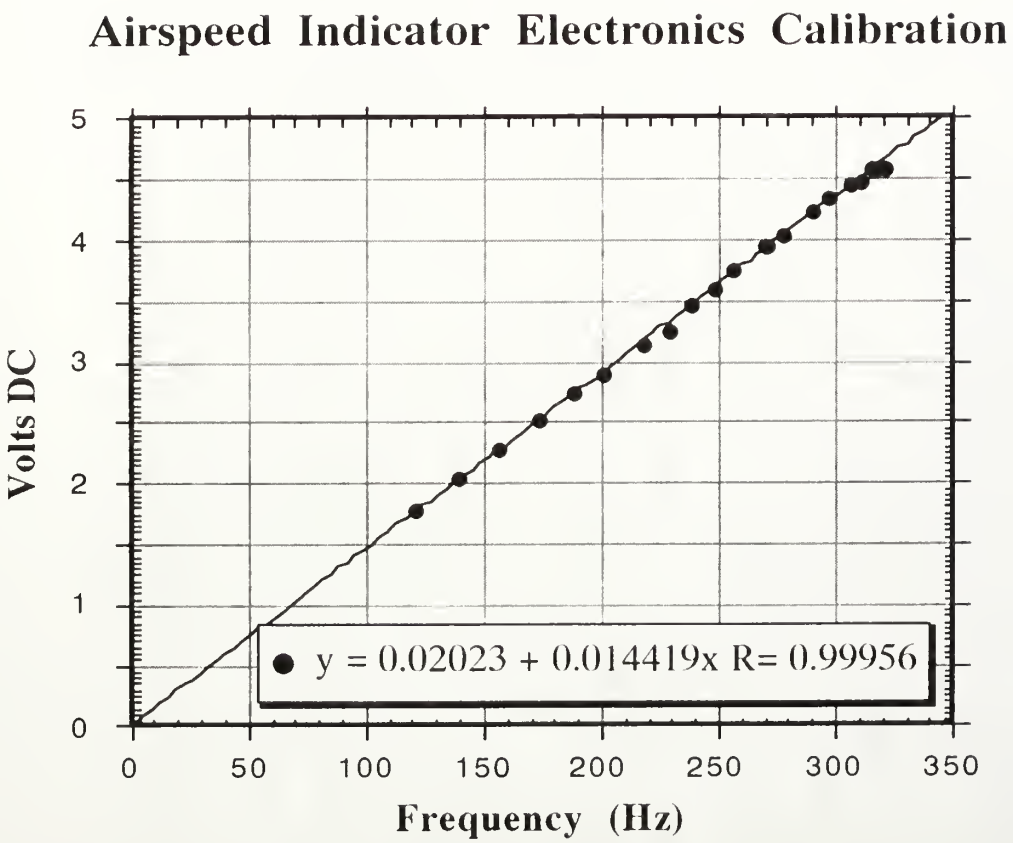
Airspeed Indicator Electronics Calibration
Volts DC
Frequency (Hz)
y = 0.02023 + 0.014419x R= 0.99956
0
1
2
3
4
5
0
50
100
150
200
250
300
350

REFERENCES

1. Murri, D.G. and Rao, D.M., *Exploratory Studies of Actuated Forebody Strakes for Yaw Control at High Angles of Attack*, AIAA Paper 87-2557, 1987.

2. McAtee, T.P., *Agility in Demand, Aerospace America*, Vol. 26, No.5, May 1988.

3. Dorn, M.D., *Aircraft Agility: The Science and the Opportunities*, AIAA Paper 89-2015, August 1989.

4. Herbst, W.B., *Future Fighter Technologies*, Journal of Aircraft, Vol. 17, No. 8, Article No. 80-4077, August 1980.

5. Gilbert, W.P., Nguyen, L.T.,and Gera, J., *Control Research in the NASA High-Alpha Technology Program*, AGARD Fluid Dynamics Panel Symposium on Aerodynamics of Combat Aircraft Control and of Ground Effects, October 1989.

6. Raney, D.L. and Batterson, J.G., *Lateral Stability Analysis for X-29A Drop Model Using System Identification Methodology*, NASA Technical Memorandum 4108, 1989.

7. Schefter, J., X-31: *How They're Inventing a Radical New Way to Fly*, Popular Science, February 1989.

8. Reznick, S.G., and Flores, J., *Strake-Generated Vortex Interactions for a Fighter-Like Configuration*, Journal of Aircraft, Vol. 26, No. 4, April 1989.

9. Tavella, D.A., Schiff, L.B., and Cummings, R.M., *Pneumatic Vortical Flow Control at High Angles of Attack*, AIAA 90-0098, January 1990.

10. Kandebo, S.W., *STOL/Maneuvering Technology Demonstrator to Explore In-Flight Thrust Reversing*, Aviation Week & Space Technology, March 26, 1990.

11. Deets, D.A. and Brown, L.E., *Experience with HiMAT Remotely Piloted Research Vehicle - An Alternate Flight Test Approach*, AIAA Paper 86-2754, October 1986.

12. *Israelis Flight Test Jet-Powered RPV Fitted With Thrust-Vectoring Nozzles*, Aviation Week & Space Technology, May 8,1987.

13. Salmons, J.D., *Developmental Flight Testing of a Half Scale Unmanned Air Vehicle*, Master's Thesis, Naval Postgraduate School, Monterey, California, September 1990.

14. Cleaver, C.M., *Development of an Unmanned Air Research Vehicle for Supermaneuverablitiy Studies*, Master's Thesis, Naval Postgraduate School, Monterey, California, March 1990.

INITIAL DISTRIBUTION LIST

		No. Copies
1.	Defense Technical Information Center Cameron Station Alexandria, VA 22304-6145	2
2.	Library, Code 0142 Naval Postgraduate School Monterey, CA 93943-5100	2
3.	Chairman, Code AA Department of Aeronautics and Astronautics Naval Postgraduate School Monterey, CA 93953-5000	1
4.	Professor Richard M. Howard, Code AA/Ho Department of Aeronautics and Astronautics Naval Postgraduate School Monterey, CA 93953-5000	2
5.	Lcdr Michael J. Gallagher 13565 S. 18th Ave. Lemoore, CA 93245	1
6.	Lcdr Chris Cleaver 1501 Crystal Drive, Apt. 1034 Arlington, VA 22202	1
7.	Mr. Richard J. Foch Naval Research Laboratory Code 5712 4555 Overlook Avenue, S.W. Washington, D.C. 20374	1
8.	Mr. Thomas Momiyama and Mr. Benjy Neumann Naval Air Systems Command Air-931K Washington, D.C. 20361	1

9. Mr. Dav id Lewis 1
UAV-Joint Project Office
Naval Air Systems Command
Code PEO (CU)-UDI
Washington, D.C. 20361-1014

10. Tom Christian, Code ME/TC 1
Department of Mechanical Engineering
Naval Postgraduate School
Monterey, CA 93953-5000

11. Mr. Mike Callaway 1
3245 Tenley Drive
San Jose, CA 95148

Thesis
G140427 Gallagher
c.1 Development of telemetry for the agility flight test of a radio controlled fighter model.